List of Suggested Reviewers or Reviewers Not To Include (optional)

SUGGESTED REVIEWERS:
Not Listed

REVIEWERS NOT TO INCLUDE:
Not Listed

Pursuant to PAPPG Chapter II.C.1.e., each PI, co-PI, and other senior project personnel identified on a proposal must provide collaborator and other affiliations information to help NSF identify appropriate reviewers.(v.4/21/2017)

Please complete this template (e.g., Excel, Google Sheets, LibreOffice), save as .xlsx or .xls, and upload directly as a Fastlane Collaborators and Other Affiliations single copy doc.
Do not upload .pdf.

There are four tables:
A: Your Name & Affiliation(s);
B: PhD Advisors/Advisees (all);
C: Collaborators;
D: Co-Editors;
E: Relationships

List names as Last Name, First Name, Middle Initial. Additionally, provide email, organization, and department (optional) to disambiguate common names.

Fixed column widths keep this sheet one page wide; if you cut and paste text, set font size at 10pt or smaller, and abbreviate, where necessary, to make the data fit.

To insert *n* blank rows, select *n* row numbers to move down, right click, and choose Insert from the menu.
You may fill-down (crtl-D) to mark a sequence of collaborators, or copy affiliations. Excel has arrows that enable sorting. "Last active" dates are optional, but will help NSF staff easily determine which information remains relevant for reviewer selection.

Table A: List your Last Name, First Name, Middle Initial, and organizational affiliation (including considered affiliation) in the last 12 months.

A	Your Name:	Your Organizational Affiliation(s), last 12 r	Last Active Date
	Vadas, Sharon L	NorthWest Research Assoc.	Current

Table B: List names as Last Name, First Name, Middle Initial, and provide organizational affiliations, if known, for the following.

G: Your PhD Advisor(s)
T: All your PhD Thesis Advisees
P: Your Graduate Advisors

to disambiguate common names

B	Advisor/Advisee Name:	Organizational Affiliation	Optional (email, Department)
G:	Kolb, Edward W.	University of Chicago	Dean Physical Sciences Division
T:			
P:	Kolb, Edward W.	University of Chicago	Dean Physical Sciences Division

Table C: List names as Last Name, First Name, Middle Initial, and provide organizational affiliations, if known, for the following.

A: Co-authors on any book, article, report, abstract or paper (with collaboration in last 48 months; publication date may be later).

C: Collaborators on projects, such as funded grants, graduate research or others (in last 48 months).

to disambiguate common names

C	Name:	Organizational Affiliation	Optional (email, Department)	Last Active

A:	Aponte, N.	Arecibo Observatory		12/19/13
A:	Azeem, Irfan	Atmospheric & Space Technology Res. Assoc.		present
C:	Azeem, Irfan	Atmospheric & Space Technology Res. Assoc.		present
A:	Bageston, J.V.	Universidade Federal de Campina Grande, Brazil		2/4/16
A:	Baggaley, W.	University of Canterbury, New Zealand		4/4/13
A:	Baumgardner, J.	Boston University		4/4/13
A:	Becker, Erich	Leibnitz Institute of Atmospheric Physics		present
C:	Bhatt, Asti	SRI International		present
C:	Bishop, Rebecca	The Aerospace Corporation		present
A:	Bishop, Rebecca	The Aerospace Corporation		6/22/15
A:	Buriti, R.A.	Universidade Federal de Campina Grande, Brazil		2/4/16
A:	Chen, Chris	University of Colorado		10/14/16
A:	Chu, Xinzhao	University of Colorado		present
C:	Chu, Xinzhao	University of Colorado		present
A:	Clemmons, James	Aerospace Corporation		6/22/15
C:	Cosgrove, Russel	SRI International		present
A:	Crowley, Geoff	Atmospheric & Space Technology Res. Assoc.		5/7/17
A:	Davidson, Ryan	Virginia Tech		6/22/15
C:	Earle, Gregory	Virginia Tech		present
A:	Earle, Gregory	Virginia Tech		6/22/15
A:	Fanelli, Lucy	Virginia Tech		6/22/15
A:	Filgueira, S.	Universidade Federal de Campina Grande, Brazil		2/4/16
A:	Fish, Chad	Virginia Tech		6/22/15
A:	Fritts, David	GATS Inc.		2/14/13
A:	Garg, Vidur	Virginia Tech		6/22/15
A:	Ghosh, Alex	University of Illinois at Urbana-Champaign		6/22/15
A:	Gobbi, D.	Instituto Nacional de Pesquisas Espaciais		2/4/16
A:	Harmon, Robert	Wesleyan University		6/20/14
A:	Hernandez, G.	University of Washington		4/4/13
A:	Jagannatha, Bindu	University of Illinois at Urbana-Champaign		6/22/15
A:	Kawamura, S.	Nat. Inst. Inform. & Comm. Tech., Japan		10/24/13
A:	Kroeker, Erik	University of Illinois at Urbana-Champaign		6/22/15
A:	Leite, D.	Universidade Federal de Campina Grande, Brazil		2/4/16
A:	Li, Haoyu	University of Colorado		10/14/16
A:	Lieberman, Ruth	GATS Inc.		6/27/14
A:	Liu, Han-Li	NCAR/HAO division		6/27/14
A:	Lu, Xian	Clemson University		10/14/16
A:	Makela, Jonathan	University of Illinois at Urbana-Champaign		2/8/17
A:	Marquis, Peter	Virginia Tech		6/22/15
A:	Martin, Daniel	Virginia Tech		6/22/15
A:	Medeiros, A	Universidade Federal de Campina Grande, Brazil		2/4/16
A:	Milliff, R.F.	University of Colorado		9/28/15
A:	Murayama, Y.	Nat. Inst. Inform. & Comm. Tech., Japan		10/24/13
A:	Nakamura, Takuji	National Institute of Polar Research, Tokyo		10/1/16
A:	Nicolls, M.J.	SRI International		9/28/15
A:	Noel, Stephen	Virginia Tech		6/22/15
A:	Orr, Cameron	Virginia Tech		6/22/15
A:	Otsuka, Y.	Nagoya University, Japan		10/24/13
A:	Paulino, Igo	Universidade Federal de Campina Grande, Brazil		2/4/16
A:	Robertson, Robert	Virginia Tech		6/22/15
A:	Shiokawa, Kazuo	Nagoya University, Japan		10/24/13
A:	Smith, John	University of Colorado		10/14/16
A:	Smith, Steve	Boston University		4/4/13
A:	Sobral, J.H.A.	Instituto Nacional de Pesquisas Espaciais		2/4/16

A:	Sulzer, Michael	Arecibo Observatory		12/19/13
A:	Suzuki, Hidehiko	Meiji University		6/20/14
A:	Suzuki, Shin	Nagoya University, Japan		10/24/13
C:	Swenson, Gary	retired, formerly University of Illinois		present
A:	Swenson, Gary	retired, formerly University of Illinois at Urbana-Champaign		5/22/17
A:	Takahashi, Hisao	Instituto Nacional de Pesquisas Espaciais		2/4/16
A:	Westerhoff, J.	University of Illinois at Urbana-Champaign		6/22/15
A:	Wrasse, C	Instituto Nacional de Pesquisas Espaciais		2/4/16

Table D: List editorial board, editor-in-chief and co-editors with whom you interact. An editor-in-chief should list the entire editorial board.

B: Editorial board: Name(s) of editor-in-chief and journal (in past 24 months).

E: Other Co-Editors of journals or collections with whom you directly interacted (in past 24 months).

to disambiguate common names

D	Name:	Organizational Affiliation	Journal/Collection	Last Active
B:				
E:				

Table E: List persons for whom a personal, family, or business relationship would otherwise preclude their service as a reviewer.

R: Additional names for whom some relationship would otherwise preclude their service as a reviewer.

to disambiguate common names

D	Name:	Organizational Affiliation	Optional (email, Department)	Last Active
R:	Becker, Erich	Leibnitz Institute of Atmospheric Physics		present

Pursuant to PAPPG Chapter II.C.1.e., each PI, co-PI, and other senior project personnel identified on a proposal must provide collaborator and other affiliations information to help NSF identify appropriate reviewers.(v.4/21/2017)

Please complete this template (e.g., Excel, Google Sheets, LibreOffice), save as .xlsx or .xls, and upload directly as a Fastlane Collaborators and Other Affiliations single copy doc.
Do not upload .pdf.

There are four tables:
A: Your Name & Affiliation(s);
B: PhD Advisors/Advisees (all);
C: Collaborators;
D: Co-Editors;
E: Relationships

List names as Last Name, First Name, Middle Initial. Additionally, provide email, organization, and department (optional) to disambiguate common names.

Fixed column widths keep this sheet one page wide; if you cut and paste text, set font size at 10pt or smaller, and abbreviate, where necessary, to make the data fit.

To insert *n* blank rows, select *n* row numbers to move down, right click, and choose Insert from the menu.
You may fill-down (crtl-D) to mark a sequence of collaborators, or copy affiliations. Excel has arrows that enable sorting.
"Last active" dates are optional, but will help NSF staff easily determine which information remains relevant for reviewer selection.

Table A: List your Last Name, First Name, Middle Initial, and organizational affiliation (including considered affiliation) in the last 12 months.

A	Your Name:	Your Organizational Affiliation(s), last 12 r	Last Active Date
	Becker, Erich	Leibniz Institute of Atmospheric Physics (cu	Current
		NWRA/CoRA (considered affiliation)	Current

Table B: List names as Last Name, First Name, Middle Initial, and provide organizational affiliations, if known, for the following.

G: Your PhD Advisor(s)
T: All your PhD Thesis Advisees
P: Your Graduate Advisors

to disambiguate common names

B	Advisor/Advisee Name:	Organizational Affiliation	Optional (email, Department)
G:	Obermeier, Frank	Technische Universität Bergakademie Freib	frank.obermeier.imfd.tu-freiberg.de
T:	Can, Serhat	Leibniz Institute of Atmospheric Physics	serhat@iap-kborn.de
T:	Kirsch, Annekatrin	Leibniz Institute of Atmospheric Physics	kirsch@iap-kborn.de
T:	Mai, Matthäus	Leibniz Institute of Atmospheric Physics	mai@iap-kborn.de
T:	Schlutow, Mark	Frei Universität Berlin	mark.schlutow@fu-berlin.de
T:	Sommerfeld, Bastian	Leibniz Institute of Atmospheric Physics	sommerfeld
T:	Brune, Sebastian	University of Hamburg	sebastian.brune@uni-hamburg.de
T:	Knöpfel, Rahel	Leibniz Institute of Atmospheric Physics	knoepfel@iap-kborn.de
T:	Schoon, Lena	Leibniz Institute of Atmospheric Physics	schoon@iap-kborn.de
T:	Senf, Fabian	Leibniz Institut of Tropospheric Research	senf@tropos.de
P:	Großmann, Siegfrid	University of Marburg, retired	

Table C: List names as Last Name, First Name, Middle Initial, and provide organizational affiliations, if known, for the following.

A: Co-authors on any book, article, report, abstract or paper (with collaboration in last 48 months; publication date may be later).

C: Collaborators on projects, such as funded grants, graduate research or others (in last 48 months).

to disambiguate common names

C	Name:	Organizational Affiliation	Optional (email, Department)	Last Active
C:	Avsarkisov, Victor	Leibniz Institute of Atmospheric Physics		10/26/17
C:	Bothe, Oliver	Helmholtz-Zentrum Geesthacht		5/31/14
C:	Can, Serhat	Leibniz Institute of Atmospheric Physics		10/26/17
C:	Chau, Jorge L.	Leibniz Institute of Atmospheric Physics		10/26/17
A:	Chen, Cao	University of Colorado		12/4/17
C:	Chu, Xinzhao	University of Colorado		11/3/17
A:	Chu, Zinzhao	University of Colorado		12/4/17
A:	Dörnbrack, Andreas	IPA, DLR Oberpfaffenhoren		12/4/17
A:	Eden, Carsten	University of Hamburg		10/27/17
C:	Eden, Carsten	University if Hamburg		10/27/17
A:	Fong, Weichun	University of Colorado		12/4/17
C:	Gabriel, Axel	Leibniz Institute of Atmospheric Physics		10/27/17
C:	Gassmann, Almut	Leibniz Institute of Atmospheric Physics		10/25/17
A:	Gerding, Michael	Leibniz Institute of Atmospheric Physics		10/26/17
C:	Grygalashvyly, Mykhaylo	Leibniz Institute of Atmospheric Physics		10/26/17
A:	Harvey, V. Lynn	University of Colorado		12/4/17
A:	Hoffmann, Peter	Leibniz Institute of Atmospheric Physics		11/3/17
A:	Höffner, Josef	Leibniz Institute of Atmospheric Physics		10/25/17
A:	Jones, R. Michael	University of Colorado		12/4/17
A:	Kaifler, Bernd	DLR Institute for Atmospheric Physics		11/24/15
A:	Karlsson, Bodil	University of Stockholm		9/22/17
A:	Knöpfel, Rahel	Leibniz Institute of Atmospheric Physics		12/7/16
A:	Körnich, Heiner	SMHI, Norrköping, Sweden		9/8/14
A:	Latteck, Ralph	Leibniz Institute of Atmospheric Physics		10/25/17
C:	Liu, Han-Li	NCAR-HAO		9/4/17
A:	Lu, Xian	Clemson University		12/4/17
A:	Lübken, Franz-Josef	Leibniz Institute of Atmospheric Physics		10/26/17
C:	Lübken, Franz-Josef	Leibniz Institute of Atmospheric Physics		10/26/17
C:	Mai, Matthäus	Leibniz Institute of Atmospheric Physics		10/27/17
A:	Murphy, Damian	Australian Antarctic Division		9/17/16
A:	Olbers, Dirk	MARUM, Bremen		10/27/17
C:	Olbers, Dirk	MARUM, Bremen		10/27/17
A:	Placke, Manja	Leibniz Institute of Atmospheric Physics		11/26/15
A:	Pollmann, Frederike	University of Hamburg		4/20/16
C:	Püstow, Robert	Leibniz Institute of Atmospheric Physics		6/10/17
A:	Rapp, Markus	DLR Institute for Atmospheric Physics		5/12/17
A:	Roberts, Brendan R.	University of Colorado		12/4/17
A:	Schaefer-Roffs, Urs	Leibniz Institute of Atmospheric Physics		11/3/17
A:	Schlutow, Mark	Freie Universität Berlin		6/8/17
C:	Söder, Jens	Leibniz Institute of Atmospheric Physics		10/26/17
A:	Vadas, Sharon L.	NWRA/CoRA		11/3/17
C:	Viehl, Timo	Leibniz Institute of Atmospheric Physics		10/26/17
A:	Yu, Zhibin	University of Colorado		12/4/17
A:	Zhao, Jian	University of Colorado		10/26/17
A:	Zülicke, Christoph	Leibniz Institute of Atmospheric Physics		10/25/17

Table D: List editorial board, editor-in-chief and co-editors with whom you interact. An editor-in-chief should list the entire editorial board.

B: Editorial board: Name(s) of editor-in-chief and journal (in past 24 months).

E: Other Co-Editors of journals or collections with whom you directly interacted (in past 24 months).

to disambiguate common names

D	Name:	Organizational Affiliation	Journal/Collection	Last Active
B:	Rycroft, Michael	University of Cambridge	Surveys in Geophysics	6/26/17
E:				

Table E: List persons for whom a personal, family, or business relationship would otherwise preclude their service as a reviewer.

R: Additional names for whom some relationship would otherwise preclude their service as a reviewer.

to disambiguate common names

D	Name:	Organizational Affiliation	Optional (email, Department)	Last Active
R:	Vadas, Sharon L.	NWRA/CoRA		present

COVER SHEET FOR PROPOSAL TO THE NATIONAL SCIENCE FOUNDATION

PROGRAM ANNOUNCEMENT/SOLICITATION NO./DUE DATE
PD 98-1521

☐ Special Exception to Deadline Date Policy

FOR NSF USE ONLY

NSF PROPOSAL NUMBER

FOR CONSIDERATION BY NSF ORGANIZATION UNIT(S) (Indicate the most specific unit known, i.e. program, division, etc.)
AGS - GEO/ATM - Aeronomy

DATE RECEIVED	NUMBER OF COPIES	DIVISION ASSIGNED	FUND CODE	DUNS# (Data Universal Numbering System)	FILE LOCATION
				151471349	

EMPLOYER IDENTIFICATION NUMBER (EIN) OR TAXPAYER IDENTIFICATION NUMBER (TIN)
911291143

SHOW PREVIOUS AWARD NO. IF THIS IS
☐ A RENEWAL
☐ AN ACCOMPLISHMENT-BASED RENEWAL

IS THIS PROPOSAL BEING SUBMITTED TO ANOTHER FEDERAL AGENCY? YES ☐ NO ☒ IF YES, LIST ACRONYM(S)

NAME OF ORGANIZATION TO WHICH AWARD SHOULD BE MADE
NorthWest Research Associates, Incorporated

AWARDEE ORGANIZATION CODE (IF KNOWN)
4087406000

ADDRESS OF AWARDEE ORGANIZATION, INCLUDING 9 DIGIT ZIP CODE
NorthWest Research Associates, Incorporated
4118 148th Ave NE
Redmond, WA. 980525164

NAME OF PRIMARY PLACE OF PERF
NorthWest Research Associates

ADDRESS OF PRIMARY PLACE OF PERF, INCLUDING 9 DIGIT ZIP CODE
NorthWest Research Associates
3380 Mitchell Lane
Boulder ,CO ,803012245 ,US.

IS AWARDEE ORGANIZATION (Check All That Apply)
☒ SMALL BUSINESS
☒ FOR-PROFIT ORGANIZATION
☐ MINORITY BUSINESS
☐ WOMAN-OWNED BUSINESS

☐ IF THIS IS A PRELIMINARY PROPOSAL THEN CHECK HERE

TITLE OF PROPOSED PROJECT **Collaborative Research: Modeling of secondary and tertiary gravity waves from orographic gravity wave forcing and comparison with satellite observations**

REQUESTED AMOUNT	PROPOSED DURATION (1-60 MONTHS)	REQUESTED STARTING DATE	SHOW RELATED PRELIMINARY PROPOSAL NO. IF APPLICABLE
$ **389,634**	**36** months	**06/01/18**	

THIS PROPOSAL INCLUDES ANY OF THE ITEMS LISTED BELOW
☐ BEGINNING INVESTIGATOR
☐ DISCLOSURE OF LOBBYING ACTIVITIES
☐ PROPRIETARY & PRIVILEGED INFORMATION
☐ HISTORIC PLACES
☐ VERTEBRATE ANIMALS IACUC App. Date _____
PHS Animal Welfare Assurance Number _____
☒ TYPE OF PROPOSAL **Research**

☐ HUMAN SUBJECTS Human Subjects Assurance Number _____
Exemption Subsection _____ or IRB App. Date _____
☐ INTERNATIONAL ACTIVITIES: COUNTRY/COUNTRIES INVOLVED
_____
☒ COLLABORATIVE STATUS
A collaborative proposal from multiple organizations (PAPPG II.D.3.b)

PI/PD DEPARTMENT
NWRA, Boulder office

PI/PD POSTAL ADDRESS
3380 Michell Lane

Boulder, CO 80301
United States

PI/PD FAX NUMBER
303-415-9702

NAMES (TYPED)	High Degree	Yr of Degree	Telephone Number	Email Address
PI/PD NAME **Sharon L Vadas**	**PhD**	**1993**	**303-415-9701**	**vasha@cora.nwra.com**
CO-PI/PD **Erich Becker**	**PhD**	**1991**	**303-415-9701**	**becker@iap-kborn.de**
CO-PI/PD				
CO-PI/PD				
CO-PI/PD				

CERTIFICATION PAGE

Certification for Authorized Organizational Representative (or Equivalent) or Individual Applicant

By electronically signing and submitting this proposal, the Authorized Organizational Representative (AOR) or Individual Applicant is: (1) certifying that statements made herein are true and complete to the best of his/her knowledge; and (2) agreeing to accept the obligation to comply with NSF award terms and conditions if an award is made as a result of this application. Further, the applicant is hereby providing certifications regarding conflict of interest (when applicable), drug-free workplace, debarment and suspension, lobbying activities (see below), nondiscrimination, flood hazard insurance (when applicable), responsible conduct of research, organizational support, Federal tax obligations, unpaid Federal tax liability, and criminal convictions as set forth in the NSF Proposal & Award Policies & Procedures Guide (PAPPG). Willful provision of false information in this application and its supporting documents or in reports required under an ensuing award is a criminal offense (U.S. Code, Title 18, Section 1001).

Certification Regarding Conflict of Interest

The AOR is required to complete certifications stating that the organization has implemented and is enforcing a written policy on conflicts of interest (COI), consistent with the provisions of PAPPG Chapter IX.A.; that, to the best of his/her knowledge, all financial disclosures required by the conflict of interest policy were made; and that conflicts of interest, if any, were, or prior to the organization's expenditure of any funds under the award, will be, satisfactorily managed, reduced or eliminated in accordance with the organization's conflict of interest policy. Conflicts that cannot be satisfactorily managed, reduced or eliminated and research that proceeds without the imposition of conditions or restrictions when a conflict of interest exists, must be disclosed to NSF via use of the Notifications and Requests Module in FastLane.

Drug Free Work Place Certification

By electronically signing the Certification Pages, the Authorized Organizational Representative (or equivalent), is providing the Drug Free Work Place Certification contained in Exhibit II-3 of the Proposal & Award Policies & Procedures Guide.

Debarment and Suspension Certification

(If answer "yes", please provide explanation.)

Is the organization or its principals presently debarred, suspended, proposed for debarment, declared ineligible, or voluntarily excluded from covered transactions by any Federal department or agency? Yes ☐ No ☒

By electronically signing the Certification Pages, the Authorized Organizational Representative (or equivalent) or Individual Applicant is providing the Debarment and Suspension Certification contained in Exhibit II-4 of the Proposal & Award Policies & Procedures Guide.

Certification Regarding Lobbying

This certification is required for an award of a Federal contract, grant, or cooperative agreement exceeding $100,000 and for an award of a Federal loan or a commitment providing for the United States to insure or guarantee a loan exceeding $150,000.

Certification for Contracts, Grants, Loans and Cooperative Agreements

The undersigned certifies, to the best of his or her knowledge and belief, that:
(1) No Federal appropriated funds have been paid or will be paid, by or on behalf of the undersigned, to any person for influencing or attempting to influence an officer or employee of any agency, a Member of Congress, an officer or employee of Congress, or an employee of a Member of Congress in connection with the awarding of any Federal contract, the making of any Federal grant, the making of any Federal loan, the entering into of any cooperative agreement, and the extension, continuation, renewal, amendment, or modification of any Federal contract, grant, loan, or cooperative agreement.
(2) If any funds other than Federal appropriated funds have been paid or will be paid to any person for influencing or attempting to influence an officer or employee of any agency, a Member of Congress, an officer or employee of Congress, or an employee of a Member of Congress in connection with this Federal contract, grant, loan, or cooperative agreement, the undersigned shall complete and submit Standard Form-LLL, ''Disclosure of Lobbying Activities,'' in accordance with its instructions.
(3) The undersigned shall require that the language of this certification be included in the award documents for all subawards at all tiers including subcontracts, subgrants, and contracts under grants, loans, and cooperative agreements and that all subrecipients shall certify and disclose accordingly.

This certification is a material representation of fact upon which reliance was placed when this transaction was made or entered into. Submission of this certification is a prerequisite for making or entering into this transaction imposed by section 1352, Title 31, U.S. Code. Any person who fails to file the required certification shall be subject to a civil penalty of not less than $10,000 and not more than $100,000 for each such failure.

Certification Regarding Nondiscrimination

By electronically signing the Certification Pages, the Authorized Organizational Representative (or equivalent) is providing the Certification Regarding Nondiscrimination contained in Exhibit II-6 of the Proposal & Award Policies & Procedures Guide.

Certification Regarding Flood Hazard Insurance

Two sections of the National Flood Insurance Act of 1968 (42 USC §4012a and §4106) bar Federal agencies from giving financial assistance for acquisition or construction purposes in any area identified by the Federal Emergency Management Agency (FEMA) as having special flood hazards unless the:
(1) community in which that area is located participates in the national flood insurance program; and
(2) building (and any related equipment) is covered by adequate flood insurance.

By electronically signing the Certification Pages, the Authorized Organizational Representative (or equivalent) or Individual Applicant located in FEMA-designated special flood hazard areas is certifying that adequate flood insurance has been or will be obtained in the following situations:
(1) for NSF grants for the construction of a building or facility, regardless of the dollar amount of the grant; and
(2) for other NSF grants when more than $25,000 has been budgeted in the proposal for repair, alteration or improvement (construction) of a building or facility.

Certification Regarding Responsible Conduct of Research (RCR)
(This certification is not applicable to proposals for conferences, symposia, and workshops.)

By electronically signing the Certification Pages, the Authorized Organizational Representative is certifying that, in accordance with the NSF Proposal & Award Policies & Procedures Guide, Chapter IX.B. , the institution has a plan in place to provide appropriate training and oversight in the responsible and ethical conduct of research to undergraduates, graduate students and postdoctoral researchers who will be supported by NSF to conduct research. The AOR shall require that the language of this certification be included in any award documents for all subawards at all tiers.

CERTIFICATION PAGE - CONTINUED

Certification Regarding Organizational Support

By electronically signing the Certification Pages, the Authorized Organizational Representative (or equivalent) is certifying that there is organizational support for the proposal as required by Section 526 of the America COMPETES Reauthorization Act of 2010. This support extends to the portion of the proposal developed to satisfy the Broader Impacts Review Criterion as well as the Intellectual Merit Review Criterion, and any additional review criteria specified in the solicitation. Organizational support will be made available, as described in the proposal, in order to address the broader impacts and intellectual merit activities to be undertaken.

Certification Regarding Federal Tax Obligations

When the proposal exceeds $5,000,000, the Authorized Organizational Representative (or equivalent) is required to complete the following certification regarding Federal tax obligations. By electronically signing the Certification pages, the Authorized Organizational Representative is certifying that, to the best of their knowledge and belief, the proposing organization:
(1) has filed all Federal tax returns required during the three years preceding this certification;
(2) has not been convicted of a criminal offense under the Internal Revenue Code of 1986; and
(3) has not, more than 90 days prior to this certification, been notified of any unpaid Federal tax assessment for which the liability remains unsatisfied, unless the assessment is the subject of an installment agreement or offer in compromise that has been approved by the Internal Revenue Service and is not in default, or the assessment is the subject of a non-frivolous administrative or judicial proceeding.

Certification Regarding Unpaid Federal Tax Liability

When the proposing organization is a corporation, the Authorized Organizational Representative (or equivalent) is required to complete the following certification regarding Federal Tax Liability:

By electronically signing the Certification Pages, the Authorized Organizational Representative (or equivalent) is certifying that the corporation has no unpaid Federal tax liability that has been assessed, for which all judicial and administrative remedies have been exhausted or lapsed, and that is not being paid in a timely manner pursuant to an agreement with the authority responsible for collecting the tax liability.

Certification Regarding Criminal Convictions

When the proposing organization is a corporation, the Authorized Organizational Representative (or equivalent) is required to complete the following certification regarding Criminal Convictions:

By electronically signing the Certification Pages, the Authorized Organizational Representative (or equivalent) is certifying that the corporation has not been convicted of a felony criminal violation under any Federal law within the 24 months preceding the date on which the certification is signed.

Certification Dual Use Research of Concern

By electronically signing the certification pages, the Authorized Organizational Representative is certifying that the organization will be or is in compliance with all aspects of the United States Government Policy for Institutional Oversight of Life Sciences Dual Use Research of Concern.

AUTHORIZED ORGANIZATIONAL REPRESENTATIVE	SIGNATURE	DATE
NAME		

TELEPHONE NUMBER	EMAIL ADDRESS	FAX NUMBER

Project Summary

Overview:

Wind flow over orography is a prolific source of "primary" atmospheric gravity waves (GWs) called mountains waves (MWs). MWs break or reach critical levels in the lower or middle atmosphere. This process not only creates small-scale secondary GWs with horizontal wavelengths λ_H less than that of the MWs, but also creates horizontal "body forces" (i.e., horizontal accelerations localized in space and time) which excite a broad spectrum of secondary GWs with λ_H *larger* than that of the MWs. Recent wintertime modeling studies for McMurdo Station in the Antarctic (166.69° E and 77.84° S) using the PI's body force model and Co-I Becker's Kühlungsborn Mechanistic general Circulation Model (KMCM) find that: 1) MW breaking and attenuation near the stratopause excites larger-scale secondary GWs with $\lambda_H \sim 500-$thousands km, vertical wavelengths $\lambda_z \sim 10-150$ km and horizontal phase speeds $c_H \sim 50-250$ m/s; and 2) nearly all of the GWs at $z > 70$ km are secondary, not primary, GWs. Analyses of wintertime lidar data at McMurdo confirms 1) the excitation of secondary GWs near the stratopause (identified within "fishbone" structures in T'), and 2) that the inferred λ_H of the GWs in the MLT (Mesosphere and Lower Thermosphere) is much larger than that in the stratosphere.

Based on previous ray trace studies for white noise and convectively-generated GWs, it is likely that the secondary GWs excited by body forces from MW attenuation which have $c_H > 80$ m/s can propagate to $z \sim 150-300$ km, where they would dissipate and create thermospheric body forces. These forces would excite "tertiary" GWs which would propagate to higher altitudes. Because GW amplitudes grow exponentially with altitude, these secondary and tertiary GWs may significantly affect the winter thermosphere via this multi-step coupling process. This idea is strongly supported by satellite data, which show that the largest, wintertime, low-Kp, southern hemisphere GW hotspot observed by the Challenging Minisatellite Payload (CHAMP) and the Gravity Field and Ocean Circulation Explorer (GOCE) satellites at $z = 300-400$ km and $z = 250-300$ km, respectively, is near the Southern Andes Mountains. No modeling study to date has examined this multi-step coupling process and its role in the formation of this hotspot.

The **main objective of our proposed research** is to determine the effect that secondary and tertiary GWs from MW attenuation has on the thermosphere via this multi-step coupling process. Research funded by this proposal includes a unique combination of detailed, targeted modeling and data analyses studies. Specific **methods** to be employed and **research** to be pursued include:

- Extract wintertime GWs from GOCE data in the vicinity of the Southern Andes and Rocky Mountains. Determine λ_H, λ_z, c_H, intrinsic period τ_{Ir} and propagation directions using a previously-developed method that utilizes the dissipative GW dispersion and polarization relations. Determine the GW spectral properties as functions of altitude, latitude, longitude and time. Look for correlations between the wind flow over nearby orography to the occurrence of these GWs.
- Using existing KMCM data, calculate the wintertime body forces over the Southern Andes, Antarctic Peninsula, and Rocky Mountains from MW attenuation. Calculate the excitation, propagation and dissipation of secondary and tertiary GWs using the PI's in-house body force and ray trace models. Compute the modeled secondary and tertiary GW spectra as functions of altitude, latitude and longitude;
- Compare the observed and modeled GW spectra. If there are differences, adjust the models and analysis methods until reasonable agreement is obtained.

Intellectual Merit: The proposed research will significantly advance our research community's knowledge of the transfer of momentum from orographic forcing to the thermosphere via GWs in this multi-step coupling process. This will lead to a much better understanding of the variability and structure of the thermosphere from these processes.

Broader Impacts: Because the neutral wind and density in the thermosphere is changed from this multi-step coupling process, these studies may help yield more-accurate calculations of satellite drag. To enhance scientific understanding for the general public, this research will be disseminated broadly via conference talks and peer-reviewed journal publications. This project would support the training of a graduate student and the research of a woman scientist (PI).

TABLE OF CONTENTS

For font size and page formatting specifications, see PAPPG section II.B.2.

	Total No. of Pages	Page No.* (Optional)*
Cover Sheet for Proposal to the National Science Foundation		
Project Summary (not to exceed 1 page)	1	
Table of Contents	1	
Project Description (Including Results from Prior NSF Support) (not to exceed 15 pages) **(Exceed only if allowed by a specific program announcement/solicitation or if approved in advance by the appropriate NSF Assistant Director or designee)**	15	
References Cited	9	
Biographical Sketches (Not to exceed 2 pages each)	4	
Budget (Plus up to 3 pages of budget justification)	10	
Current and Pending Support	3	
Facilities, Equipment and Other Resources	1	
Special Information/Supplementary Documents (Data Management Plan, Mentoring Plan and Other Supplementary Documents)	2	
Appendix (List below.) **(Include only if allowed by a specific program announcement/ solicitation or if approved in advance by the appropriate NSF Assistant Director or designee)**		
Appendix Items:		

*Proposers may select any numbering mechanism for the proposal. The entire proposal however, must be paginated. Complete both columns only if the proposal is numbered consecutively.

Project Description

1. Introduction

Wind flow over orography excites mountains waves (MWs) (*Holton*, 1992; *Fritts and Alexander*, 2003). If the wind is constant in time and the flow is linear, the ground-based phase speed of a MW, c_H, is zero and the solution is steady-state. MWs have been observed over the Southern Andes in South America and the Antarctic Peninsula with the Cryogenic Infrared Spectrometers and Telescopes for the Atmosphere (CRISTA) (*Eckermann and Preusse*, 1999; *Ern et al.*, 2004), the Upper Atmosphere Research Satellite Microwave Limb Sounder (UARS MLS) (*Jiang et al.*, 2002; *Wu and Jiang*, 2002), the Atmospheric Infrared Sounder (AIRS) (*Wu et al.*, 2006; *Hoffmann and Alexander*, 2009; *Alexander and Teitelbaum*, 2007, 2011; *Gong et al.*, 2012), the High Resolution Dynamics Limb Sounder (HIRDLS) and the Sounding of the Atmosphere using Broadband Emission Radiometry (SABER) (*Alexander et al.*, 2008; *Ern et al.*, 2011), the meteorological program of the Global Positioning System (GPS/MET) (*Tsuda et al.*, 2000), GPS radio occultation (*de la Torre and Alexander*, 2005), and superpressure balloons (*Vincent et al.*, 2007; *Plougonven et al.*, 2008; *Walterscheid et al.*, 2016). They have also been observed over New Zealand in the Deep Propagating Gravity Wave Experiment (DEEPWAVE) (*Fritts et al.*, 2016; *Bossert et al.*, 2015, 2017; *Heale et al.*, 2017) and near McMurdo Station in Antarctica with superpressure balloons and AIRS (*Vincent et al.*, 2007; *Hoffmann et al.*, 2013; *Hendricks et al.*, 2014).

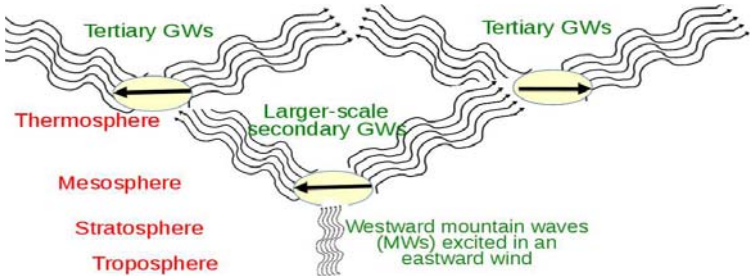

Figure 1: Schematic showing the proposed multi-step coupling mechanism between MWs, secondary GWs, and tertiary GWs. Westward MWs are excited in an eastward wind, thereby creating a stationary MW pattern. A westward body force (black arrows) is created where the MWs dissipate, which excites eastward and westward-propagating secondary GWs. The upward-propagating secondary GWs propagate into the thermosphere where they dissipate and create thermospheric body forces. These body forces then excite tertiary GWs. Only the upward-propagating secondary and tertiary GWs are shown here for clarity. (Not to scale).

MWs and their effects can be modeled in the winter stratosphere and MLT by high-resolution, GW-resolving GCMs. *Sato et al.* (2012) found stratospheric MW hotspots leeward of the Southern Andes during winter. They showed a correlation between downward energy flux in the stratosphere and orographic GW activity over the Southern Andes. They postulated that this might be due to partial wave reflection from the changing buoyancy frequency or to nonlinear processes (i.e., small-scale secondary GWs created from wave breaking), although neither possibility was deemed as entirely satisfactory. They also found orographic GWs near McMurdo in July, thereby confirming their creation by (downslope) katabatic winds at the western edge of the Ross Sea (*Watanabe et al.*, 2006). Recently, *Becker and Vadas* (2018) analyzed GWs in the stratosphere and mesosphere in the southern winter hemisphere using the high-resolution, GW-resolving KMCM. They found that westward MWs were created by eastward flow over the Southern Andes, Antarctic Peninsula and McMurdo Station from Rossby waves. During large events, MWs propagated to the stratopause region where they broke and created temporally and spatially-dependent wave drag (i.e., body forces). These events preceded strong GW events in the MLT. Importantly, they found that the GWs in the MLT propagated eastward, westward, northward and southward, with peak values of $c_H \sim 60$ m/s. They identified these GWs as secondary GWs from intermittent, localized body forces from MW breaking in the stratopause region. *Vadas et al.* (2017) calculated the spectra of secondary GWs theoretically. They found that these spectra are quite broad, and have $\lambda_H \sim 500$

to thousands km, $\lambda_z \sim 10-150$ km and $c_H \sim 50-250$ m/s. They also found that secondary GWs form "fishbone" structures in $z-t$ plots of the temperature and wind perturbations. *Vadas and Becker* (2017) analyzed the wintertime KMCM data over McMurdo during large MW events. They found that fishbone structures were common in the stratopause region, and that these structures contained larger-scale upward and downward-propagating secondary GWs with $\lambda_H \sim 1000-3000$ km and $c_H \sim 40-70$ m/s. Detailed analysis showed that these GWs were excited by horizontal body forces that were created by the breaking of MWs with $\lambda_H \sim 230$ km near the stratopause.

Because the secondary GW spectrum excited by a body force is broad (*Vadas et al.*, 2003, 2017), it is expected that many secondary GWs with $c_H > 80$ m/s can propagate to $z \sim 150-300$ km (*Vadas*, 2007), where they would dissipate from molecular viscosity or breaking. This dissipation would result in momentum deposition, which would create thermospheric body forces. Fig. 1 sketches this proposed mechanism. Here, the thermospheric body forces excite "tertiary" GWs that propagate to the middle and upper thermosphere. Because a GW's amplitude increases exponentially in z, this multi-step coupling process likely results in a significant transfer of momentum from the troposphere to the thermosphere. Although this process likely has a profound effect on the thermosphere and ionosphere, no modeling study of this process has been performed to date.

Recent observational evidence supports the occurrence of larger-scale secondary GWs in the winter MLT. GW momentum flux estimates based on meteor radar measurements east of the Southern Andes revealed a significant vertical flux of eastward momentum which could not be explained by non-orographic tropospheric GWs because of critical level filtering by the strong polar vortex (*de Wit et al.*, 2017). Indeed, *de Wit et al.* (2017) argued that these fluxes were secondary GWs excited in the stratosphere from MW breaking over the Southern Andes. Additionally, several fishbone structures in lidar data at McMurdo near the winter stratopause were shown to contain secondary GWs through detailed analyses (*Vadas et al.*, 2017). Finally, using wintertime lidar data at McMurdo, it was found that the inferred GW λ_H was much larger in the MLT than in the stratosphere (*Zhao et al.*, 2017; *Chen et al.*, 2013; *Chen and Chu*, 2017), in excellent agreement with model results (*Becker and Vadas*, 2018; *Vadas and Becker*, 2017).

The research proposed here will perform detailed model and data analysis studies. The main objectives of this research are 1) to extract individual GWs from GOCE density and cross-track winds over the Southern Andes and Rocky Mountains, and to determine λ_H, λ_z, τ_{Ir}, c_H, and their direction of propagation using the dissipative GW dispersion and polarization relations; 2) to model the secondary and tertiary GWs excited by body forces from MW breaking and attenuation over the Southern Andes, Antarctic Peninsula and Rocky Mountains, and to determine their amplitudes, λ_H, λ_z, τ_{Ir}, c_H, and their direction of propagation in the thermosphere; and 3) to compare the results from the models and data. This research targets the Southern Andes because it contains the largest quiet-time winter GW hotspot at $z = 250-300$ km. We also investigate the Rocky Mountains because it contains a large quiet-time, winter GW hotpot at midlatitudes. We will perform these studies using publicly-available GOCE, MERRA-2, HWM, and MSIS data, in-house existing KMCM data, and in-house body force and ray trace models. We are able to proceed immediately on all elements of this proposal because the PI and Co-Is have the experience, in-house mature codes and models, and data needed to complete this work. Our proposed research will lead to a much better understanding of the parameters and amplitudes of the secondary and tertiary GWs in the thermosphere from orographic forcing, and will probe the acceleration of the horizontal background wind which occurs in the thermosphere where the secondary GWs dissipate. This research will lead to a much better understanding of the transfer of momentum from orographic forcing in the troposphere to dynamical changes and variability in the thermosphere, and thus will lead to a much better understanding of the complex multi-step coupling process which likely occurs between the lower, middle and upper atmosphere through orographic forcing.

2. Current Research Status and Needs

a. Importance of gravity waves in the mesosphere and thermosphere

GWs are created from lower atmospheric sources such as wind flow over orography, deep convection, shear, wave breaking, tsunamis, etc. Because their amplitudes grow exponentially with

altitude, many GWs eventually break in the lower and middle atmosphere. Wave-breaking excites small-scale secondary GWs and wave motions (e.g. *Bacmeister and Schoeberl*, 1989; *Taylor and Hapgood*, 1990; *Walterscheid and Schubert*, 1990; *Taylor et. al.*, 1995; *Holton and Alexander*, 1999; *Fritts et al.*, 1998; *Franke and Robinson*, 1999; *Satomura and Sato*, 1999; *Nakamura et al.*, 1999; *Huang et al.*, 1992; *Prusa et al.*, 1996; *Fritts et al.*, 1998; *LeLong and Dunkerton*, 1998; *Liu et al.*, 1999; *Yamada et al.*, 2001; *Fritts et al.*, 2002; *Hecht*, 2004; *Li et al.*, 2005; *Snively and Pasko*, 2003, 2008; *Heale et al.*, 2017). Because these GWs typically cannot propagate very far before being reabsorbed into the fluid (although they may carry and transport significant momentum flux in the process (*Bossert et al.*, 2017)), they can be loosely thought of as being part of the transition to smaller scales and to turbulence.

As a result of wave breaking, momentum is deposited into the fluid on scales of order the wave packet, which is *larger* than λ_H of the breaking GW (*Vadas and Fritts*, 2002). This deposition corresponds to a horizontal body force, and results in a temporally and spatially-localized horizontal acceleration of the background wind in the direction the primary GW was propagating (*Vadas et al.*, 2003; *Fritts et al.*, 2006). The fluid responds to this imbalance by radiating larger-scale secondary GWs and creating a horizontal mean flow that contains 2 counter-rotating cells (*Vadas et al.*, 2003, 2017; *Vadas and Liu*, 2009). These secondary GWs propagate forward, backward, upward and downward away from the body force, and have a broad spectrum of horizontal scales which peaks at $\sim 2\times$ the width of the body force (*Vadas et al.*, 2003, 2017). Because these latter secondary GWs have much larger λ_H and intrinsic horizontal phase speeds c_{IH} than the small-scale secondary GWs mentioned above, they can propagate to much higher altitudes before dissipating (*Vadas*, 2007). For deep convection, this process results in the significant transfer of momentum from the troposphere to the thermosphere (*Vadas and Liu*, 2009, 2013; *Vadas et al.*, 2014). For the remainder of this proposal, secondary GWs refers to the latter, larger-scale GWs generated by body forces.

If a GW propagates above the turbopause, it dissipates from kinematic viscosity, thermal diffusivity, ion drag, and wave-induced diffusion (*Pitteway and Hines*, 1963; *Gossard and Hooke*, 1975; *DelGenio and Schubert*, 1979; *Hickey and Cole*, 1988; *Vadas and Fritts*, 2004, 2005; *Vadas*, 2007; *Miyoshi and Fujiwara*, 2008; *Yiğit et al.*, 2008; *Heale et al.*, 2017), with kinematic viscosity (ν) and thermal diffusivity (ν/Pr, where Pr ~ 0.7 is the Prandtl number) being the most important for GWs with periods $\tau_r <$ few hours. Because ν grows exponentially with altitude, every GW eventually dissipates from viscosity, although the height where this occurs depends sensitively on τ_{Ir} and λ_z (*Vadas*, 2007; *Vadas and Liu*, 2009). In particular, GWs with smaller (larger) λ_z and c_{IH} dissipate at lower (higher) altitudes (*Pitteway and Hines*, 1963; *Volland*, 1969; *Vadas*, 2007), as has been observed for λ_z (*Oliver et al.*, 1997; *Djuth et al.*, 1997, 2004). Additionally, large-amplitude GWs can break in the thermosphere (*Lund and Fritts*, 2012).

GW dissipation in the thermosphere creates thermospheric body forces (*Vadas and Liu*, 2009, 2013; *Vadas*, 2013). For deep convection, these forces peak at $z \sim 170-200$ km with amplitudes of $\sim 0.2-1.0$ m/s^2 over spatially localized regions of $\sim 100-1500$ km and time scales of $\sim 10-30$ min, and create 1) secondary GWs having $\lambda_H \sim 100-4000$ km and $c_H \sim 100-500$ m/s and 2) neutral horizontal wind perturbations of $u'_H \sim 50-200$ m/s (*Vadas and Liu*, 2009, 2013; *Vadas and Crowley*, 2010; *Vadas et al.*, 2014). *Vadas and Liu* (2009) showed that a low-latitude convective plume created secondary GWs with $\rho'/\overline{\rho} \sim 4-5\%$ at $z \sim 400$ km and [O] perturbations of $\sim$2% at $z = 300$ km, in agreement with low Kp CHAMP and DE2 satellite observations, respectively (*Bruinsma and Forbes*, 2008; *Hedin and Mayr*, 1987; *Mayr et al.*, 1990). Because deep convection is the main creator of GWs at low latitudes, *Vadas and Liu* (2009) concluded that most of the low latitude quiet-time (i.e., low Kp) $\rho'/\overline{\rho}$ and [O] perturbations measured by these satellites were likely secondary GWs generated by thermospheric body forces created by the dissipation of primary GWs from deep convection. Other studies using a parameterized orographic GW spectrum show that dissipating GWs change the zonal mean zonal winds on a global scale up to $z \sim 240$ km with accelerations as large as ~ 150 m/s/day (*Yiğit et al.*, 2009), and create zonal wind variability in the thermosphere of $\sim 100-200$ m/s (*Miyoshi and Fujiwara*, 2008). Thus, GWs from deep convection transfer significant amounts of momentum from the lower atmosphere to the thermosphere, and

thus likely play a key coupling role in this process.

b. Model for the excitation of MWs from wind flow over orography: KMCM

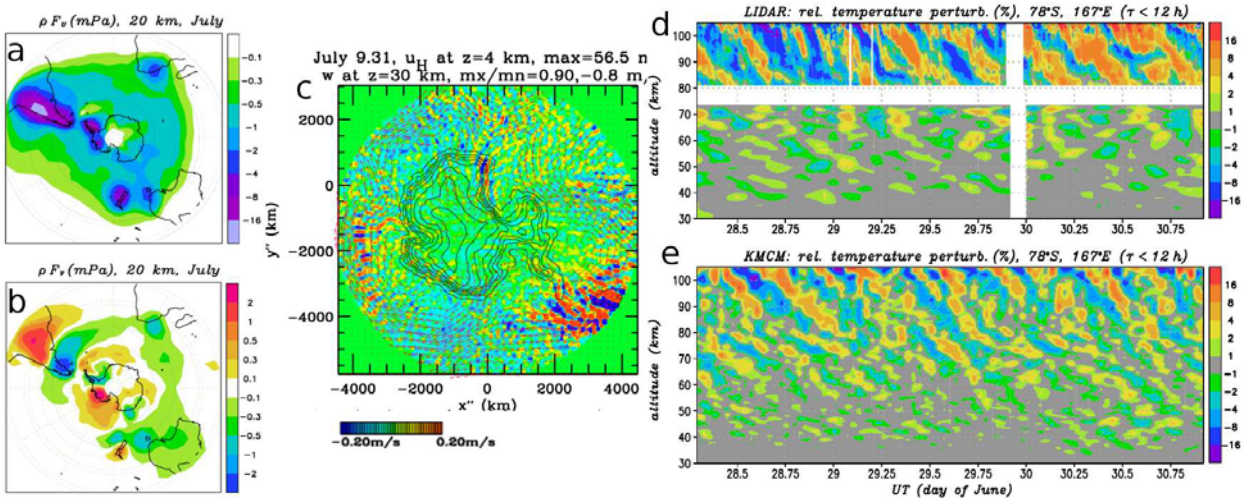

Figure 2: Zonal (a) and meridional (b) GW momentum fluxes at $z = 20$ km in July. c): The vertical velocity w on July 9.31 at $z = 30$ km (color contours) on a 2D plane parallel to the Earth's surface at McMurdo (located at $x'' = y'' = 0$). d) Ground-based lidar measurements of the temperature perturbations T' at McMurdo (with $\tau_r \leq 11$ hrs) for June 28-31 using the data from *Chen et al.* (2016). e) T' from the KMCM for GWs with $\tau_r \leq 11$ hrs for the same time period. a,b,d and e from *Becker and Vadas* (2018). c from *Vadas and Becker* (2017).

The Kühlungsborn Mechanistic general Circulation Model (KMCM) is a high-resolution, GW-resolving, free-running global circulation model (*Becker*, 2009; *Hoffmann et al.*, 2010; *Becker*, 2012; *Becker and Vadas*, 2018). It is based on a standard spectral dynamical core with a terrain-following hybrid vertical coordinate, and uses a triangular spectral truncation at total horizontal wavenumber 240 and 190 full model layers (T240L190) up to $z \sim 130$ km. The KMCM has recently been extended up to $z \sim 200$ km. The resulting horizontal and vertical grid spacings are ~ 55 km and ~ 600 m, respectively, for $z \leq 100$ km. The KMCM resolves GWs down to $\lambda_H \geq 165$ km. The KMCM includes explicit computations of radiation and the tropospheric moisture cycle (*Becker et al.*, 2015; *Becker*, 2017). Land-sea contrasts are included via orography and land-sea masks (albedo, relative humidity, heat capacity and roughness length). A simple slab ocean is included to close the surface energy budget.

Subgrid-scale parameterizations consist of a 1) local boundary diffusion scheme, 2) simple tropospheric moist convection scheme, and 3) Smagorinsky-type horizontal and vertical diffusion scheme for the whole atmosphere, with both diffusion coefficients dependent on the Richardson number, R_i, such as to give rise to wave damping when $R_i \leq 0.25$ (*Becker*, 2009). A sponge layer is included in the top 30 km via linear harmonic horizontal diffusion. The entire momentum diffusion (including the sponge layer) conserves angular momentum. The model thermosphere also includes a simple ion drag scheme. All subgrid-scale momentum tendencies are energetically balanced by the corresponding frictional heating terms (*Becker*, 2017).

Fig. 2a-b shows the zonal and meridional GW momentum fluxes at $z = 20$ km from the KMCM during the wintertime in the southern hemisphere. Strong MW activity is seen over the Southern Andes, Antarctic Peninsula, and New Zealand, in agreement with observations (e.g. *Jiang et al.*, 2002; *Alexander and Teitelbaum*, 2011). Fig. 2c shows a snapshot of the vertical wind at $z = 30$ km from the KMCM. The horizontal wind excites MWs over the Antarctic Peninsula ($x'' \sim 3000$ km, $y'' \sim -4000$ km) and McMurdo ($x'' = y'' = 0$). Fig. 2d shows lidar observations of the temperature perturbations T' at McMurdo in June. Large-amplitude GWs with $\tau_r = 3 - 10$ hrs are present in the stratosphere and MLT. Fig. 2e shows the corresponding KMCM results. Good agreement is seen between the model results and lidar observations in τ_r, λ_z, and amplitudes.

c. 3D Model: GW excitation from body forces

Our GW excitation model from body forces solves the linear, f-plane, Boussinesq or compressible fluid equations for horizontal body forces which vary smoothly over the duration χ (*Vadas and Fritts*, 2001, 2013; *Vadas*, 2013). The compressible solutions are necessary to calculate the amplitudes of GWs with $|\lambda_z| > 30$ km. The width, depth and time scale of a body force are related to the characteristics of the dissipating/breaking GW packet that created the force.

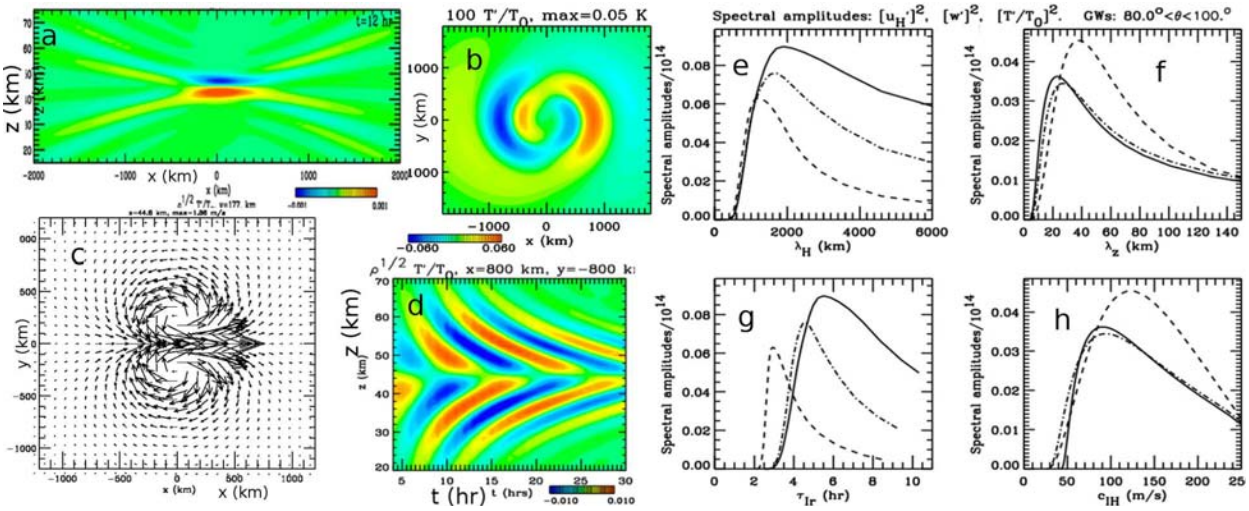

Figure 3: Secondary GWs and mean responses to a zonal body force centered at $z = 45$ km that starts at $= 0$, has a full width and depth of 800 and 8 km, respectively, and a duration of 2 hr (a-d, e-h) and 6 hr (d). a) $\sqrt{\overline{\rho}}T'/\overline{T}$ at $t = 12$ hr, where $\overline{\rho}$ and $\overline{T}$ are the background density and temperature. b) $100T'/\overline{T}$ at $t = 4$ hr and $z = 60$ km. c) The mean horizontal velocity response at $z = 45$ km showing the 2 counter-rotating cells. The arrows are proportional to the maximum amplitude of 1.7 m/s. d) $\sqrt{\overline{\rho}}T'/\overline{T}$ versus z and t at $x = 800$ km, $y = -800$ km. e-h) Spectra of secondary GWs with azimuths $80 - 100°$. Solid, dash and dash-dot lines show horizontal velocity, vertical velocity and temperature spectra as functions of λ_H (d), $|\lambda_z|$ (e), τ_{Ir} (f), and c_{IH} (g). From *Vadas et al.* (2017).

Fig. 3a shows a zonal-vertical slice of $\sqrt{\overline{\rho}}T'/\overline{T}$ (where $\overline{\rho}$ and $\overline{T}$ are the background density and temperature, respectively) of the secondary GWs and the mean response created by a Gaussian zonal body force centered at $z = 45$ km with full width and depth of 800 km and 8 km, respectively, and a 2 hr duration. This force is in an isothermal atmosphere with zero background wind, and is modeled after a body force studied by *Vadas and Becker* (2017) which occurred ~ 400 km northwest of McMurdo after a MW packet with $\lambda_x \sim 230$ km broke. The secondary GWs propagate upward, downward, eastward and westward. Fig. 3b shows a horizontal slice of $100T'/\overline{T}$ at $t = 4$ hr and $z = 60$ km. The secondary GWs form partial concentric rings, and have the same amplitudes in the eastward and westward directions. Fig. 3c shows that 2 counter-rotating cells in the horizontal plane are created by this force, with the flow being in the direction of the force at its center. Fig. 3d shows that the secondary GWs create a fishbone structure in a $z - t$ plot of $\sqrt{\overline{\rho}}T'/\overline{T}$. The knee of this structure, $z_{\rm knee}$, occurs at the center of the body force ($z_{\rm knee} = 45$ km here). Fig. 3e-h shows 1D spectra of the excited secondary GWs. The horizontal velocity and temperature spectra peak at twice the full width of the force. Some of these secondary GWs have $|\lambda_z| > 40$ km and intrinsic horizontal phase speeds $c_{IH} > 80$ m/s, which enable them to propagate well into the thermosphere before dissipating (*Vadas*, 2007). To model the propagation of secondary GWs in an atmosphere with realistic wind and temperatures, we employ ray tracing (see the next section).

d. 3D GW Ray trace model

Our 3D GW ray trace model includes horizontally, vertically and temporally-varying background winds and temperatures, critical level filtering, and evanescence (*Vadas*, 2007; *Vadas et al.*, 2009a; *Vadas et al.*, 2012, 2014, 2015; *Azeem et al.*, 2017; *Vadas and Crowley*, 2017). It also includes parameterized GW breaking (including self and wave-wave interactions) via Lindzen's lin-

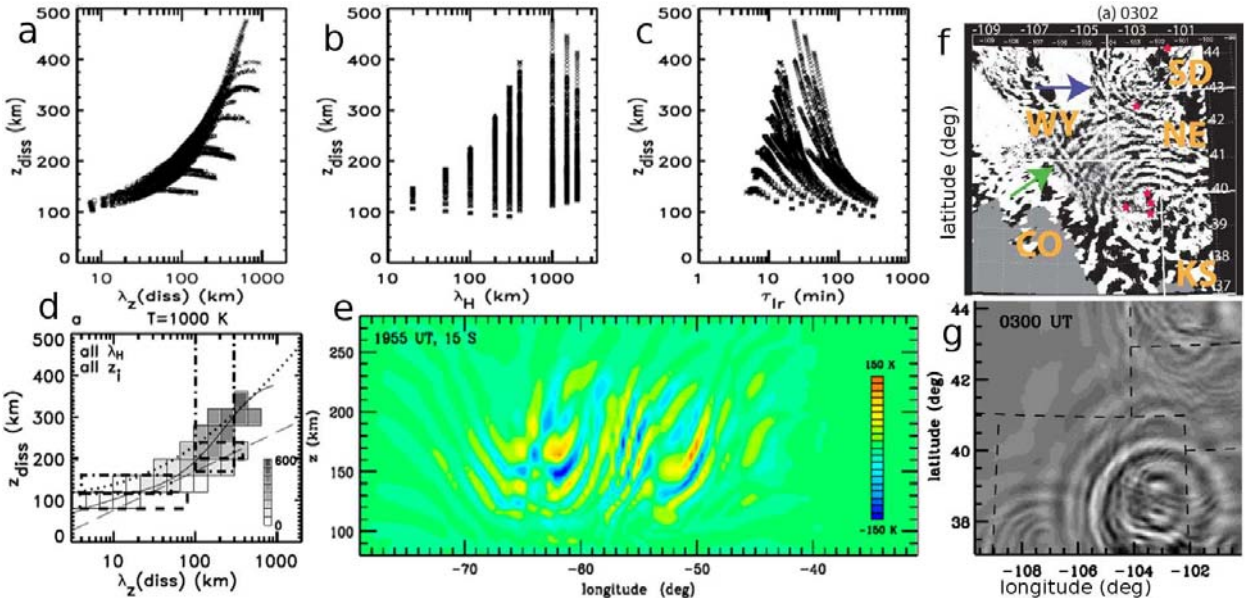

Figure 4: a-c) The dissipation altitude of GWs, $z_{\rm diss}$ (i.e., where the momentum flux is maximum), as a function of λ_z, λ_H, and τ_{Ir}. Launch altitudes include $z_i = 0$, 120, and 180 km. d) $z_{\rm diss}$ as a function of λ_z for a thermosphere with $\overline{T} = 1000$ K. We overlay observational results of *Djuth et al.* (1997, 2004) as dash-dot boxes and *Oliver et al.* (1997) as long dash lines. a-d) from *Vadas* (2007). e) T' for the primary GWs from deep convection over Brazil on 01 October 2005 at 15 S and 19:55 UT. T' is calculated via the PI's convective plume and ray trace models. From *Vadas and Liu* (2013). f) OH perturbations at Yucca Ridge, CO, USA on 8 Sept 2005 at 03:02 UT. g) Modeled OH perturbations at the same time using the PI's convective plume and ray trace models. f-g) from *Vadas et al.* (2012).

ear saturation scheme (*Lindzen*, 1981; *Smith et al.*, 1987), realistic dissipation in the thermosphere from molecular viscosity and thermal diffusivity (*Vadas and Fritts*, 2005), and the change of a GW's ground-based frequency due to rapidly-varying background winds (*Eckermann and Marks*, 1996). It includes the increase in a GW's amplitude from the decrease in background density and its decrease from dissipation, as well as the integration of each GW's phase along its ray path. The computed GW momentum fluxes and parameters (including phases) are saved in cells as functions of (x, y, z, t). The GW dissipative polarization relations are then used to reconstruct the GW field (*Vadas and Fritts*, 2009; *Vadas et al.*, 2009b; *Vadas et al.*, 2012; *Vadas and Liu*, 2009, 2013; *Vadas*, 2013). This is not a DNS; instead, the polarization relations are applied to the average GW parameters and momentum fluxes in each cell to reconstruct the GW field in the mesosphere and thermosphere (e.g. *Vadas and Fritts*, 2009).

Fig. 4a-c shows the results of ray tracing a white noise spectrum of GWs from launch altitudes of $z_i = 0$, 120 and 180 km in zero background wind. λ_z increases exponentially with altitude in the thermosphere at the GW dissipation altitude, $z_{\rm diss}$. At $z = 280$ km, $\lambda_z \sim 100 - 300$ km, $\lambda_H \sim 100$ to thousands of km, and $\tau_{Ir} \sim 10$ min to hours. Fig. 4d shows that the GW ray trace results of λ_z agree well with Arecibo Observatory and the MU radar observations up to the mid-thermosphere. Fig. 4e shows the result of ray tracing GWs excited by deep convection over Brazil into the thermosphere. Most of the GWs dissipate by $z \sim 250$ km, with the peak occurring at $z \sim 190$ km (*Vadas and Liu*, 2009). At $z = 250$, the primary GWs have $\rho'/\overline{\rho}$ ~1-2% and the secondary GWs (excited at $z \sim 190$ km) have $\rho'/\overline{\rho}$ ~5-16% (*Vadas and Liu*, 2013). Fig. 4f shows the OH airglow perturbations from GWs excited by deep convection in the USA. Fig. 4g shows the corresponding OH perturbations from the PI's models. Good agreement is seen.

e. GOCE measurements

The European Space Agency (ESA) GOCE mission was dedicated to precisely measure the gravity field of Earth. It was launched into polar 0600/1800 local time (LT) Sun-synchronous orbit

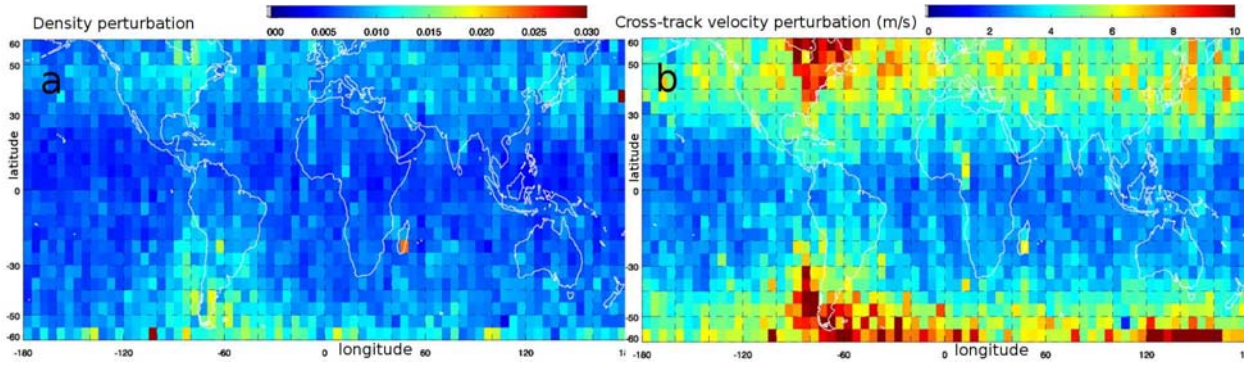

Figure 5: Perturbations from GOCE waves with $\lambda_{track} \leq 1000$ km. a) $\sqrt{\Sigma_i(\rho_i'/\overline{\rho}_i)^2}$, b) $\sqrt{\Sigma_i(u'_{xtrack})^2}$, where the sum is over all the "i" events in each $5^\circ \times 5^\circ$ bin. (Courtesy of Suang Yu and Co-I Yue)

on 17 March 2009 and reentered on 11 November 2013. Air density and cross-track winds are derived independently from the accelerometer data and thruster accelerations based on modeling of radiation, satellite area and orientation (*Bruinsma*, 2013; *Doornbos*, 2016; *Doornbos et al.*, 2013, 2014; *Bruinsma et al.*, 2014). The data processing involves conversion of ion thruster activation data to accelerations, iterative adjustment of wind direction and air density inputs of an aerodynamic model of the satellite, until the model aerodynamic accelerations match the observations.

Before mid 2012, GOCE's orbit was stable at $z \sim 260 - 290$ km. Afterward, it's orbit dropped to 250 km in August 2012, to 245 km in November 2012, to 240 km in February 2013, and to 230 km in May 2013. During this time period the LT of GOCE's orbit slowly drifted from 0600/1800 to 0730/1930 LT. Additionally, the density (wind) errors (included in the data files) decreased on average from about 2.5% ($30 - 40$ m/s) during 2009-2010 to 1.5% ($15 - 20$ m/s) until August 2012, then remained at $\sim 1\%$ ($7 - 12$ m/s) until November 2013. The useful latitude range of the GOCE data is $\pm 60^\circ$ with ~ 15 orbits per day, with each orbit separated by 24° longitude.

To extract GWs with along-track horizontal scales of $\lambda_{track} \leq 1000$ km, we first calculate "background" latitudinal profiles of the density, $\overline{\rho}$, and cross-track wind, $\overline{u}_{xtrack}$, by applying a low-pass Butterworth filter to the GOCE density ρ and cross-track wind u_{xtrack}. We then calculate the density and cross-track wind perturbations, $\rho' = \rho - \overline{\rho}$ and $u'_{xtrack} = u_{xtrack} - \overline{u}_{xtrack}$, respectively. Fig. 5a-b shows the averaged global density and cross-track wind perturbation amplitudes, respectively, in June-August 2010 for both ascending and descending nodes, binned on a $5^\circ \times 5^\circ$ grid. Here, we only include data with Kp < 3 to minimize contamination from GWs created by large geomagnetic activities. The largest wintertime hotspot of $|\rho'|/\overline{\rho}$ ~few % and $|u'_{xtrack}| \sim 5 - 10$ m/s occurs in the region of the Southern Andes. Additionally, there is a summertime hotspot near the east coast of North America, presumably due to deep convection. This result is in rough agreement with *Forbes et al.* (2016) and *Liu, Pedatella et al.* (2017).

f. Method to determine intrinsic parameters of GWs from in-situ measurements

Gross et al. (1984) used the phase shifts and amplitude ratios of the O and N_2 perturbations to estimate the propagation directions (to within 180°) of GWs observed by the AE-C satellite. *Innis and Conde* (2002) analyzed DE2 satellite measurements of the vertical velocity perturbation w', u'_{xtrack}, the inferred height change h, and the inferred pressure p' to determine the GW propagation directions to within 90°. If u'_{xtrack} was in phase with p', then the GW propagated eastward. And if h led w' by 90°, then the GW propagated in the same direction as the spacecraft. ω_{Ir} was then determined via $h = w'/i\omega_{Ir}$. Although *Innis and Conde* (2002) included compressibility, they did not take into account viscous dissipation.

Vadas and Nicolls (2012) generalized these approaches by including compressibility and realistic thermospheric viscosity in the GW dissipative dispersion and polarization relations (originally derived by *Vadas and Fritts*, 2005). With this method, the phase shifts and amplitude ratios between 2 or more components of a GW (i.e., between w', u'_{xtrack}, ρ', and T') are used to determine

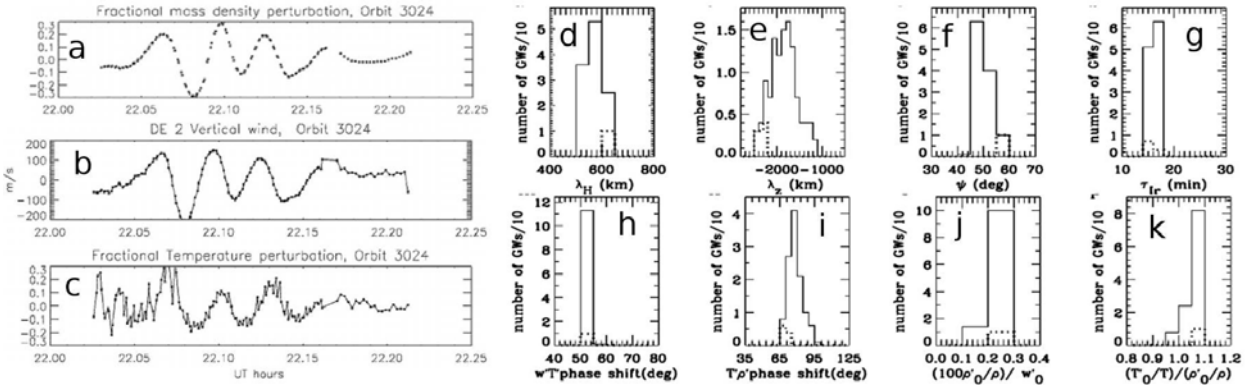

Figure 6: DE2 WATS and NACS data for Orbit 3024, 1982 day 053. a-c): Fractional mass density, vertical velocity and fractional neutral temperature perturbations, respectively. From *Innis and Conde* (2002). d-k): GW solutions for the 5 independent constraints (solid lines) as a function of d-k): λ_H, λ_z, ψ, τ_{Ir}, w'-T' phase shift, T'-ρ' phase shift, $(100\rho'_0/\overline{\rho})/w'_0$ and $(T'_0/\overline{T})/(\rho'_0/\overline{\rho})$. Dotted lines show the best-fit solutions. From *Vadas and Nicolls* (2012).

λ_H, λ_z, ω_{Ir}, and the GW propagation direction. This method was applied to a DE2 GW (see next paragraph), to a GW observed in the thermosphere by Fabry-Perot interferometers over Alaska (*Nicolls et al.*, 2012), and to GWs observed by several lidars in Colorado (*Lu et al.*, 2017).

Using the phase shifts and amplitude ratios between w', T' and ρ', *Vadas and Nicolls* (2012) reanalyzed a DE2 GW originally analyzed by *Innis and Conde* (2002) (see Fig. 6a-c). Fig. 6d-k shows the GW solutions where the phase shifts, amplitude ratios, and along-track distance between perturbation maxima, $\lambda_{\rm track}$, equaled the observed values for a reasonable range of atmospheric parameters. We see that the solution is confined to a relatively-narrow region in parameter space. The best-fit GW has $\lambda_H = 600 - 625$ km, $|\lambda_z| \sim (2200 - 2500)$ km, azimuth $\psi = -(55 - 60)^\circ$, and $\tau_{Ir} \sim 16 - 17$ min. Since w', ρ' and T' were measured independently by DE2, this overlap was considered remarkable, and provided an excellent test and validation of this method—namely that GW dissipative theory can be utilized to calculate the intrinsic parameters and propagation directions of GWs from in-situ satellite measurements.

g. Secondary GWs from MW breaking and GOCE measurements

Given the current model status, data, and methods discussed above, we now discuss preliminary studies and science needs necessary for a better understanding of the multi-step coupling process between MW breaking in the lower atmosphere and secondary/tertiary GWs in the thermosphere.

g.1 Secondary GWs from MW breaking at McMurdo

Fig. 7a-f shows horizontal slices of w above McMurdo on July 9.5 (i.e., 12 UT on July 9) from the KMCM at z = 16, 30, 42, 46, 60 and 76 km, respectively. Here we have transformed the data to a 2D plane tangent to Earth at McMurdo (*Vadas and Becker*, 2017). We see that quasi-stationary MWs with $\lambda_H \simeq 230$ km propagate to $z \sim 40 - 60$ km, where they break and dissipate. No MWs are present at $z = 76$ km. The divergence of the zonal momentum flux (i.e., the zonal body forces) are also shown. For $z \sim 40 - 60$ km, zonal forces are strong 300-1000 km north of McMurdo. Fig. 7g shows that fishbone structures occur a few hrs later. Fig. 7h-j show the GWs from Fig. 7g filtered for $165 < \lambda_H < 700$ km, $700 < \lambda_H < 3000$ km and $3000 < \lambda_H < 5050$ km, respectively. Most of the fishbone structure is comprised of larger-scale GWs with $\lambda_H \sim 700$ to 3000 km. Through detailed analyses, *Vadas and Becker* (2017) found that this fishbone structure was comprised of secondary GWs excited by a zonal body force at $z \sim 46$ km created from MW breaking 400 km northwest of McMurdo on July 9.5.

Fig. 8a shows the $T'\sqrt{\overline{\rho}/\overline{\rho}_0}$ above McMurdo at $z = 60 - 100$ km on July 8-11 from the KMCM. Fig. 8b-d shows the same perturbations, but filtered for GWs with $165 < \lambda_H < 1000$ km, $1000 < \lambda_H < 3000$ km, and $3000 < \lambda_H < 5050$ km, respectively. Above $z > 70$ km, nearly all of the GWs have $1000 < \lambda_H < 3000$ km; therefore, the GWs at $z = 70 - 100$ km have much larger λ_H

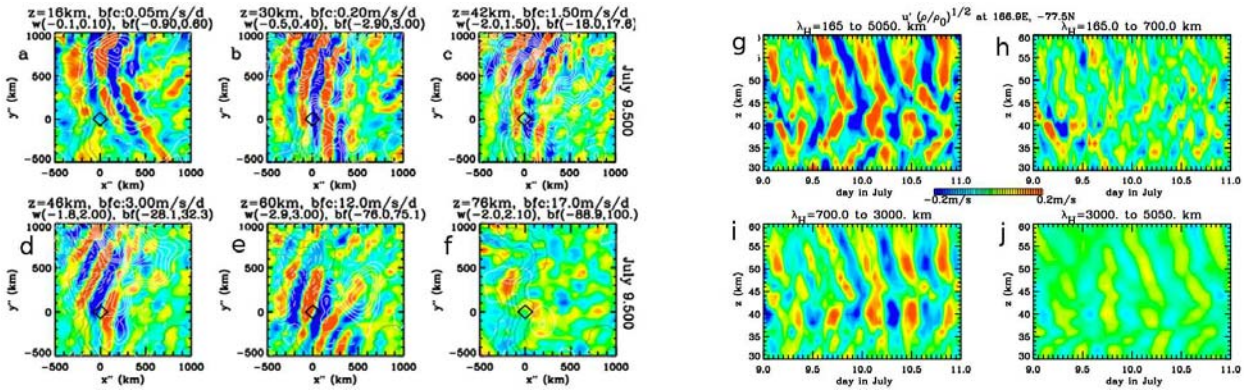

Figure 7: a-f) w from the KMCM on a 2D plane tangent to Earth at McMurdo (black diamond) at $z = 16$, 30, 42, 46, 60 and 76 km on July 9.5. Blue to red show $\pm.02$, .1, .4, .6, 1 and 1 m/s, respectively. Solid (dashed) lines show the positive (negative) zonal body force in .05, .2, 1.5, 3, 12, and 17 m/s/day intervals. g) $u'\sqrt{\overline{\rho}/\overline{\rho}_0}$ at McMurdo with $165 < \lambda_H < 5050$ km. $\overline{\rho}_0$ is the value of $\overline{\rho}$ at 0E, 90°S and $z = 5$ km on July 3.0. h-j) As in g) but for GWs with $165 < \lambda_H < 700$ km, $700 < \lambda_H < 3000$ km, and $3000 < \lambda_H < 5050$ km. From *Vadas and Becker* (2017).

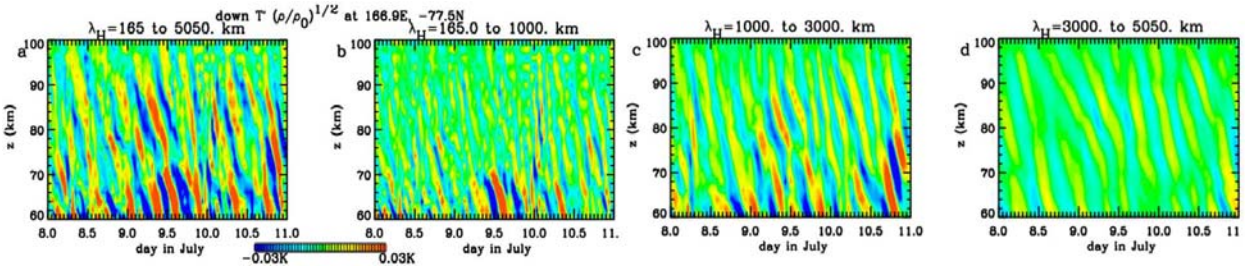

Figure 8: $T'\sqrt{\overline{\rho}/\overline{\rho}_0}$ at McMurdo from the KMCM for the GWs with downward phase progression. a) GWs with $165 < \lambda_H < 5050$ km. b) GWs with $165 < \lambda_H < 1000$ km. c) GWs with $1000 < \lambda_H < 3000$ km. d) GWs with $3000 < \lambda_H < 5050$ km. From *Vadas and Becker* (2017).

than near the stratopause; this is because the GWs in the MLT are secondary, not primary, GWs. This KMCM result is confirmed by wintertime lidar observations at McMurdo; *Zhao et al.* (2017) inferred that the GWs at $z = 30 - 50$ km had $\lambda_H \sim 350 - 500$ km, whereas *Chen et al.* (2013) and *Chen and Chu* (2017) inferred that the GWs at $z = 70 - 100$ km had $\lambda_H \sim 400 - 4000$ km.

Secondary GWs have now been identified in several fishbone structures from lidar data at McMurdo via detailed analyses (*Vadas et al.*, 2017). Fig. 9a shows $\sqrt{\overline{\rho}}T'/\overline{T}$ on 18 June 2014, and Fig. 9b shows the same data, but only for waves with $\tau_r \leq 11$ hr. At 5-26 UT and $z \sim 30 - 50$ km, constructive and destructive interference is seen for GWs with upward and downward phase progression; a possible fishbone structure is apparent with $z_{\rm knee} \simeq 43$ km. Fig. 9c shows the result after removing GWs with downward phase progression at $z < z_{\rm knee}$ and upward phase progression at $z > z_{\rm knee}$. These removed GWs have relatively large amplitudes at $z < z_{\rm knee}$. *Vadas et al.* (2017) found that these removed GWs have $\tau_r = 8.1 \pm 0.5$ hr and $|\lambda_z| = 4.7 \pm 0.5$ km. Fig. 9d shows the possible secondary GWs, obtained by subtracting Fig. 9c from Fig. 9b. The fishbone structure is visible for $z = 30 - 50$ km at 5-26 UT. The GWs below $z_{\rm knee}$ have $\tau_r = 9.5 \pm 0.6$ h and $|\lambda_z| = 13.6 \pm 1.2$ km, while those above $z_{\rm knee}$ have $\tau_r = 8.3 \pm 0.5$ h and $|\lambda_z| = 13.6 \pm 2.2$ km; thus $|\lambda_z|$ and τ_r are similar below and above $z_{\rm knee}$ for the GWs in the fishbone structure, thereby meeting an important criterion to identify these GWs as secondary GWs. Additionally, the possible secondary GWs at $z > z_{\rm knee}$ are not continuations of the removed GWs because $|\lambda_z|$ is much larger for the possible secondary GWs. Finally, using background winds from MERRA-2, *Vadas et al.* (2017) showed that the possible secondary GWs with upward/downward phase progression are downward/upward-propagating GWs. (Merra-2 is the Modern-Era Retrospective analysis for Research and Applications, Version

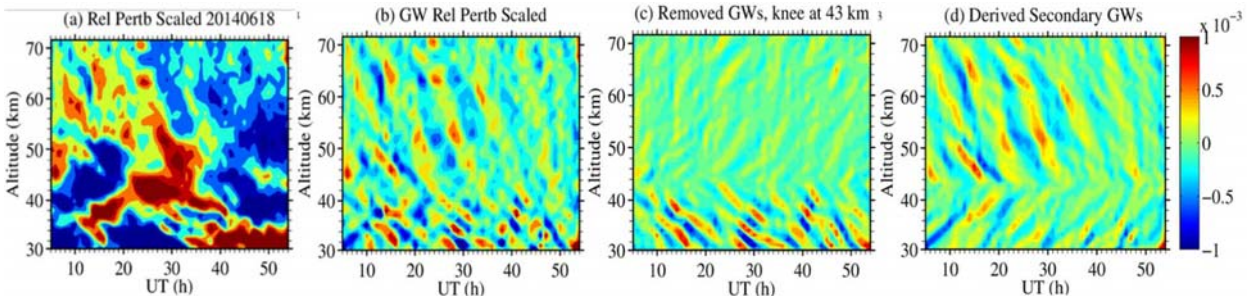

Figure 9: Lidar observations at McMurdo. a) Density-scaled temperature perturbations, $\sqrt{\overline{\rho}}T'/\overline{T}$, on 18 June 2014. b) As in a), but only retain GWs with periods ≤ 11 hr. c) Removed GWs obtained by selecting GWs from b) with upward phase progression for $z > z_{\rm knee}$ and downward phase progression for $z < z_{\rm knee}$. Here, $z_{\rm knee} = 43$ km. d) Derived secondary GWs, obtained by subtracting (c) from (b). From *Vadas et al.* (2017).

2, available at https : //gmao.gsfc.nasa.gov/reanalysis/MERRA − 2/.) After additional analyses involving other criteria, *Vadas et al.* (2017) concluded that the GWs in the fishbone structure in Fig. 9d were likely secondary GWs excited by a body force centered at $z \simeq 43$ km.

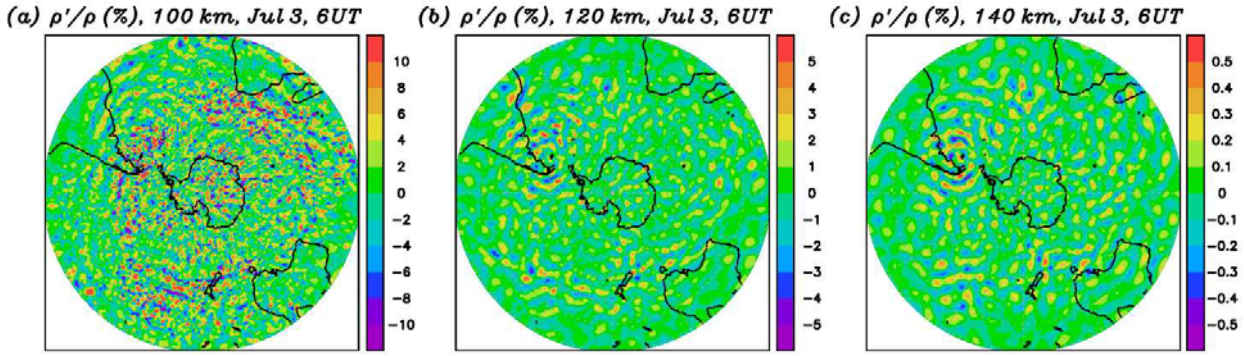

Figure 10: KMCM density perturbations, $\rho'/\overline{\rho}$, on 3 July at 6 UT for horizontal scales < 1000 km over the Southern Andes at a) $z = 100$ km, b) 120 km and c) 140 km. From Becker and Vadas, in preparation.

The KMCM result that most of the wintertime GWs at McMurdo in the MLT are secondary GWs is a stunning result, and highlights the importance of this multi-step coupling process in understanding the energetics and dynamics of the polar southern winter MLT. Additionally, GWs are excited in the thermosphere from thermospheric body forces created where primary GWs from deep convection dissipate (*Vadas and Liu*, 2009, 2013; *Vadas et al.*, 2014). Thus, we extrapolate that tertiary GWs are likely created in the thermosphere by thermospheric body forces where some of the secondary GWs break or dissipate from molecular viscosity. Indeed, Fig. 10 shows $\rho'/\overline{\rho}$ from the KMCM at $z = 100$, 120 and 140 km one day after a strong MW event occurred in the Southern Andes. Importantly, concentric ring-like structures (similar to Fig. 3b) are seen at $z = 120$ and 140 km over the southern Andes with $\lambda_H \sim 800 - 1000$ km. Because their radii are small, these are likely tertiary GWs created by thermospheric body forces.

Figs. 6-10 raise the following questions: Do some of the secondary GWs from MW breaking propagate to $z = 250 - 300$ km? Are tertiary GWs excited in the thermosphere, and do they propagate to $z = 250 - 300$ km? What are the amplitudes, scales and azimuths of the secondary and tertiary GWs at $z \sim 250 - 300$ km? Do they agree with the GOCE GWs? *Vadas* (2007) showed that white noise GWs with $100 < \lambda_H < 3000$ km and $c_{IH} > 200$ m/s can propagate to $z \sim 250 - 300$ km. Since some of the secondary GWs have these properties (see Fig. 3e,h), it is likely that at least some of the secondary GWs propagate to $z \sim 250 - 300$ km. The tertiary GW spectrum is currently unknown.

To date, no GW modeling studies have been performed to determine the role that secondary and tertiary GWs from MW breaking and attenuation play in the formation of the wintertime hotspot in the GOCE data at $z = 250 - 300$ km (see Fig. 5). To understand their role and to answer these questions, we need to calculate the secondary GWs excited by body forces from MW breaking in the KMCM. We then need to ray trace these secondary GWs into the thermosphere, calculate the body forces where these secondary GWs dissipate, calculate the excited tertiary GWs, and ray trace these GWs to higher altitudes. Finally, we need to compare the amplitudes and scales of the secondary and tertiary GWs at $z \sim 250 - 300$ km with that from the GOCE GWs. Doing these studies would result in a much better understanding of the role that this multi-step coupling process has in the formation of the wintertime hotspot in the thermosphere over the Southern Andes.

g.2 Determination of intrinsic GW parameters from GOCE measurements

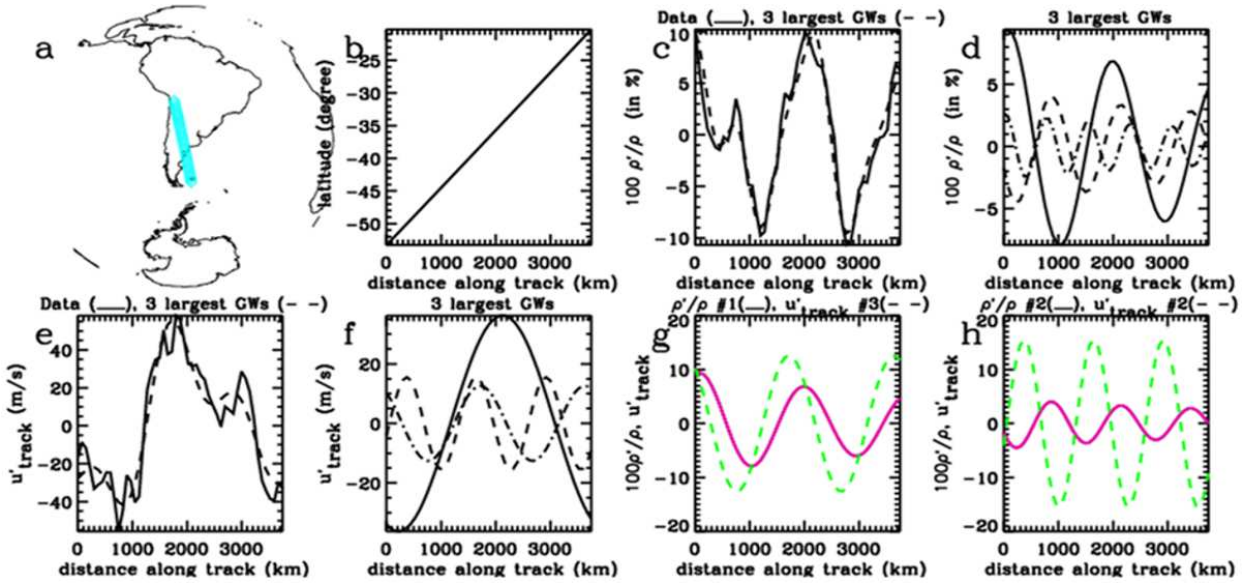

Figure 11: a) GOCE ascending path on orbit # 13 on 5 July 2010 (blue). b) Distance along the track as a function of latitude. c) $100\rho'/\overline{\rho}$ after subtracting the linear fit (solid). The sum of $100\rho'/\overline{\rho}$ for the 3 sine waves (dashed). d) $100\rho'/\overline{\rho}$ for the 3 sine waves (solid, dashed, and dashed-dotted). e) u'_{xtrack} after subtracting the linear fit (solid). The sum of u'_{xtrack} for the 3 sine waves (dashed). f) u'_{xtrack} for the 3 sine waves (solid, dashed, and dashed-dotted). g) $100\rho'/\overline{\rho}$ (solid) and u'_{xtrack} (dashed) for GW#1. h) Same as g), but for GW#2. (Vadas, Yue, et al., in preparation.)

Fig. 11 shows a preliminary analysis of the GOCE data on 5 July 2010 at 23 UT. At this time, Kp < 3, and GOCE was traveling northward over South America at $z \sim 270 - 280$ km. We subtract linear trends from ρ and u_{xtrack}, then fit the 3 largest-amplitude sine waves to ρ' and u'_{xtrack} separately. Fig. 11c,e shows the linearly-detrended data and the sum of the 3 sine waves for ρ and u_{xtrack}, respectively. The individual sine waves are shown in Fig. 11d,f for $\rho'/\overline{\rho}$ and u'_{xtrack}, respectively. We then match the sine waves for ρ' and u'_{xtrack} having similar λ_{track}; here, λ_{track} is the distance between maxima along the satellite track (see Fig. 12a). Fig. 11g shows $100\rho'/\overline{\rho}$ and u'_{xtrack} for GW#1. For this GW, $\lambda_{track} = 1947$ and 1945 km, respectively. The phase shift between ρ' and u'_{xtrack} is $-55°$. Because u'_{xtrack} peaks at the same location as u'_H (where u'_H is the GW horizontal velocity perturbation), and because u'_{xtrack} peaks before ρ', this GW propagated opposite to the satellite direction (i.e., southward) (see Fig. 2 of *Vadas and Nicolls*, 2012). Additionally, the sign of u'_{xtrack} at the peak relative to the ρ' peak indicates that this GW propagated eastward. Fig. 11h shows $100\rho'/\overline{\rho}$ and u'_{xtrack} for GW#2. The distance between maxima for $\rho'/\overline{\rho}$ and u'_{xtrack} are $\lambda_{track} = 1197$ and 1196 km, respectively. The phase shift between ρ' and u'_{xtrack} is 22°. In contrast to GW#1, we find that GW#2 propagated northwestward.

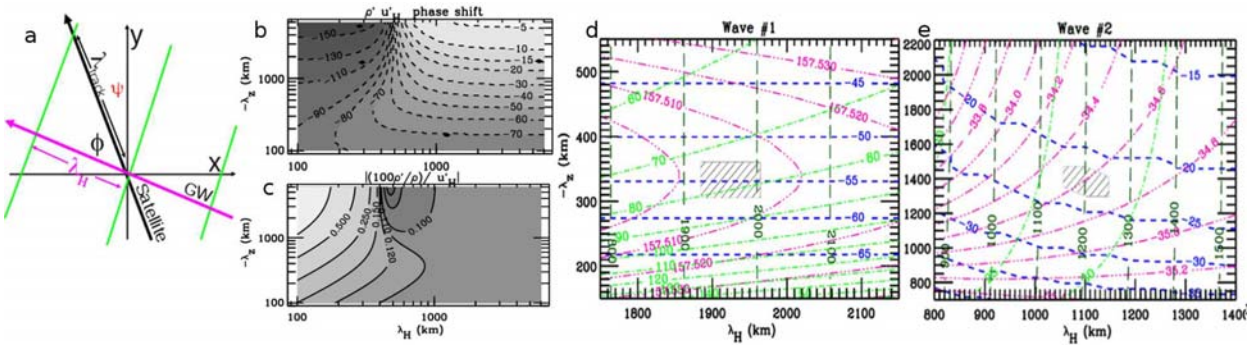

Figure 12: a) Satellite track (black arrow), GW propagation direction (purple arrow), GW lines of constant phase (green lines). λ_{track} is the distance between GW maxima along the satellite track. ϕ is the angle between the satellite track and the GW direction. ψ is the azimuth of the satellite track (east of north). b) The phase shift between ρ' and u'_{xtrack}. c) Amplitude ratio $(\rho'_0/\overline{\rho})/u'_{H0}$. d) Result for GOCE GW#1. The phase shift between ρ' and u'_{xtrack} in degrees (dash blue), λ_{track} in km (long dashed dark green), intrinsic period τ_{Ir} in min (dash-dot green) and GW azimuth (dash-dot-dot-dot pink). The hatched box shows the overlap of the observed phase shift and λ_{track}. e) Same as d) but for GW#2. (Vadas, Yue *et al.*, in preparation.)

We now estimate the intrinsic parameters for GWs#1 and 2 using GW dissipative theory. Fig. 12a sketches a canonical satellite track and GW propagation direction. Since $z = 275$ km and $\overline{\rho} = 1 \times 10^{-8}$ gm/m^3, we estimate $\overline{T} = 650$ K, $\nu = 10^{-6}$ m^2/s, $\gamma = 1.63$, molecular weight $X_{MW} = 16$ gm/mole, buoyancy period $\tau_B = 10.9$ min, density scale height H = 37 km, and sound speed $c_s = 744$ m/s (*Vadas*, 2007; *Vadas and Crowley*, 2017). Fig. 12b-c shows the resulting GW phase shifts and amplitude ratios between ρ' and u'_H for this atmosphere using the formalism from *Vadas and Nicolls* (2012). Fig. 12d shows a blow-up of the region of interest for GW#1. The best-fit solution (hatched region) for GW#1 is that it propagated southeastward with an azimuth of $\psi \sim 157°$, $\lambda_H = 1900-1950$ km, $|\lambda_z| = 300-360$ km, $\tau_{Ir} = 70-85$ min, and intrinsic horizontal phase speed $c_{IH} = 370-470$ m/s. Here we used

$$\sin\phi = \frac{u'_{xtrack,meas}}{u'_{H,0}} = \frac{u'_{xtrack,meas}}{(100\rho'_{meas}/\overline{\rho})} \left[\frac{(100\rho'_0/\overline{\rho})}{u'_{H,0}}\right] \qquad \text{and} \qquad \lambda_H = \lambda_{\rm track}\cos\phi, \tag{1}$$

where the ratio in square brackets is determined from the GW dissipative polarization relations (i.e., Fig. 12c), and the subscript "*meas*" refers to the measured values. Fig. 12e shows the result for GW#2. The best-fit solution for GW#2 is that it propagated northwestward with $\psi \sim -34°$, $\lambda_H = 1050-1150$ km, $|\lambda_z| = 1300-1500$ km, $\tau_{Ir} = 25-30$ min, and $c_{IH} = 580-770$ m/s. Because c_{IH} is larger than the sound speed c_s in the middle atmosphere for both GWs, GWs#1 and 2 must have been created in the thermosphere (*Vadas and Crowley*, 2010). Thus we tentatively conclude that GWs#1 and 2 were tertiary GWs created from the dissipation of (different sets of) secondary GW spectra, and that these secondary GW spectra were created independently from MW breaking and attenuation over the Southern Andes and the Antarctic Peninsula, respectively.

Figs. 11-12 demonstrate that a complete set of GW parameters (i.e., amplitude, τ_{Ir}, λ_H, λ_z, c_{IH}, and azimuth) can be obtained from the GOCE data. Additionally, Fig. 12 strongly suggests that GWs#1 and 2 were tertiary GWs from MW breaking over the Southern Andes and the Antarctic Peninsula (since $c_{IH} > c_s$ in the lower/middle atmosphere). This suggests that momentum and energy were transferred from orographic forcing to the thermosphere via this multi-step coupling process. Because this process involves the dissipation of secondary GWs in the thermosphere, the background neutral horizontal wind will be accelerated in spatially and temporally-localized patches above strong MW events (similar to what occurs above regions of deep convection (*Vadas and Liu*, 2009)). Such processes could significantly alter the winds in the winter middle thermosphere; rather than being dominated by slow, large-scale tidal motions, the neutral winds might have significant variability on times scales of hours and horizontal scales of $500-4000$ km. There-

fore, investigating this multi-step coupling process is likely to lead to an increased understanding of the dynamics and variability of the thermosphere.

To date, we have only made preliminary analyses of 2 GOCE GWs, and we have not compared our results with modeling studies. What is needed are detailed analyses of GOCE GWs in regions of interest. We need to determine their amplitudes and intrinsic parameters. We then need to compare these GWs with the GWs from the modeling studies. Performing these studies would allow us to better-understand the role that orographic forcing plays in the variability and dynamics of the thermosphere through this multi-step coupling process.

3. Proposed Research, Activities and Experiment Plan

Our proposed research involves extracting GWs from the GOCE data during the winter over the Southern Andes and Rocky Mountains. We propose to determine their intrinsic parameters using the dissipative GW polarization and dispersion relations. We propose to model the secondary GWs excited by body forces from MW breaking and attenuation over the Southern Andes, Antarctic Peninsula and Rocky Mountains from the KMCM. We propose to ray trace these secondary GWs into the thermosphere, calculate the thermospheric body forces, model the excited tertiary GWs, and ray trace them to higher altitudes. We propose to compare the parameters and amplitudes of these GWs with those extracted from the GOCE data. Our proposed research requires the use of publicly-available GOCE density and cross-track wind data, and data from publicly-available MERRA-2, HWM (Horizontal Wind Model, (*Drob et al.*, 2015)), and MSIS (NRLMSISE-00 Atmosphere Model, available at https : //ccmc.gsfc.nasa.gov/modelweb/models/nrlmsise00.php). Our proposed research requires the use of our in-house ray trace and body force models, which have been employed extensively in previous research and run on the desktop machines at NWRA/CoRA (e.g. *Vadas and Fritts*, 2001, 2005, 2009; *Vadas*, 2007, 2013; *Vadas et al.*, 2009a,b; *Vadas et al.*, 2012, 2014; *Vadas and Liu*, 2009, 2013; *Vadas and Crowley*, 2010, 2017; *Vadas and Nicolls*, 2012; *Nicolls et al.*, 2012). Our proposed research also requires the use of 12 months of in-house, existing KMCM data which extends to $z = 100$ km (*Becker and Vadas*, 2018; *Vadas and Becker*, 2017). The KMCM has also been employed extensively in previous research (*Becker*, 2009; *Hoffmann et al.*, 2010; *Becker*, 2012; *Becker et al.*, 2015; *Becker*, 2017). Our proposed research also requires Co-I Yue's extensive experience extracting GWs from satellite data (*Yue et al.*, 2013, 2014a,b; *Liu, Yue et al.*, 2017; *Rong et al.*, 2017). Thus we are fully equipped to carry out the research proposed here, because we have the relevant experience, data and models available to us.

a. Extracting GWs from GOCE data and determining their intrinsic parameters

For this research, we propose to use the publicly-available V1.5 GOCE density and cross-track wind data. This data is available from November 2009 to October 2013, and has already been downloaded by Co-I Yue. We propose to focus on days and times when Kp < 3 and GOCE overpassed near the Southern Andes and the Rocky Mountains. To extract individual GWs from GOCE, we propose to remove the linear trends from the density and cross track wind along the satellite track. We then propose to fit 3-5 of the largest sine waves to the density and cross-track wind perturbations separately, similar to Fig. 11. We propose to match the sine waves from ρ' and u'_{xtrack} having similar λ_{track}, and calculate their amplitudes and phase shifts. For each GW, we propose to determine its intrinsic parameters (λ_H, λ_z, τ_{Ir} and c_{IH}) and direction of propagation using the GW dissipative dispersion and polarization relations, similar to Sec. 2g.2 and Fig. 12. We propose to analyze the GWs from an estimated ~ 100 GOCE overpasses near the Southern Andes and Rocky Mountains. We propose to compile our GW spectra as functions of altitude, latitude, longitude, and time. Finally, we propose to investigate possible correlations between GOCE GW events with MW events using the wind over nearby mountains from MERRA-2. In performing these studies, we propose to:

- extract GWs from GOCE data during magnetically-quiet times (Kp < 3) during the winter over regions near the Southern Andes and the Rocky Mountains;
- determine the GW amplitudes, direction of propagation and intrinsic parameters (λ_H, λ_z, τ_{Ir} and c_{IH}) as functions of altitude, latitude, longitude, and time;
- investigate possible correlations between GOCE GWs and MW events.

Performing these studies will result in a much better understanding of the amplitudes, scales and azimuths of the GWs which contribute to the wintertime hotspots in the GOCE data.

b. Modeling the GW multi-step coupling process due to orographic forcing

We propose to use existing KMCM data to calculate the body forces that occur where MWs break and attenuate during the winter over the Southern Andes, Antarctic Peninsula and Rocky Mountains. We propose to determine the excited secondary GW spectra from a range of representative body forces using our in-house body force model. We propose to ray trace these secondary GWs (with their phases) into the thermosphere using our in-house ray trace model. We propose to reconstruct the GW field in the thermosphere via inserting the average GW momentum fluxes, wavevectors and phases into the dissipative GW polarization relations (*Vadas and Fritts*, 2005, 2009; *Vadas et al.*, 2015). We then propose to use these reconstructed GW fields to calculate the thermospheric body forces which result where the secondary GWs dissipate (*Becker*, 2004; *Vadas and Fritts*, 2006; *Vadas and Liu*, 2009). We propose to calculate the tertiary GW spectra excited by a range of representative thermospheric body forces using our in-house body force model. We propose to ray-trace these GWs to higher altitudes. For ray tracing, we propose to construct canonical background atmospheres via publicly-available MERRA-2, HWM and NRLMSISE-00 data. We propose to include the large winds in the MLT (e.g. *Larsen*, 2002; *Larsen et al.*, 2003; *Nicolls et al.*, 2014), and to vary the winds and temperatures through reasonable ranges to estimate the range in our results (similar to *Vadas et al.* (2009a)).

We propose to determine the amplitudes, propagation directions, λ_H, λ_z, τ_{Ir} and c_{IH} of the secondary and tertiary GWs as functions of altitude, latitude, longitude and time. We propose to compare the amplitudes, parameters and scales of these GWs at $z \simeq 250 - 300$ km with those extracted from the GOCE data. If there are discrepancies between the observational and modeling results, we propose to iterate our results until the model and observational results agree reasonably well. In doing this research, we propose to

• Analyze the KMCM data in the wintertime during MW events over the Southern Andes, Antarctic Peninsula, and Rocky Mountains. Calculate the body forces where these MWs break;

• Calculate the secondary GW spectra excited by a range of representative body forces. Ray trace these GWs into the thermosphere, and calculate the thermospheric body forces which result where they dissipate. Calculate the tertiary GW spectra excited by a range of representative thermospheric body forces. Ray trace these GWs to higher altitudes.

• Determine the amplitudes, propagation directions, λ_H, λ_z, τ_{Ir} and c_{IH} for the secondary and tertiary GWs separately as functions of altitude, latitude, longitude and time. Determine the results for weak and strong MW events.

• Compare the model results with GOCE-derived GWs.

• Estimate the amplitudes and scales of the variability of the neutral wind in the thermosphere due to the thermospheric body forces from the dissipation of secondary GWs.

Performing these studies will result in a much better understanding of the multi-step coupling process which transfers momentum from orographic forcing in the troposphere to GWs and variability in the thermosphere.

4. Anticipated Research Schedule, Objectives, Summary of Tasks, and Work Plan

Here we display a summary of our research objectives, tasks, and work plan over the full term of the proposed research effort.

Year 1:

• Calculate the body forces in the KMCM over the winter Southern Andes and Antarctic Peninsula, calculate the excited secondary GWs, ray trace them into the thermosphere, calculate the thermospheric body forces, calculate the tertiary GWs and ray trace them to higher altitudes. Determine the amplitudes and parameters of the secondary and tertiary GWs as functions of altitude, latitude, longitude and time. (Drs. Vadas and Becker)

• Analyze the GOCE data during the winter in regions near the Southern Andes. Extract 3-5 sine waves for each event. (Graduate student and Dr. Yue)

• Determine the intrinsic parameters and azimuth for each GOCE GW. (Dr. Vadas)

• Present results at a conference, and prepare and publish a paper for a peer-reviewed journal. (Drs. Vadas, Yue and Becker and graduate student)

Year 2:

• Same as year 1, but for new cases over the Southern Andes and Antarctic Peninsula. Completion of the study over the Southern Andes and Antarctic Peninsula. (Drs. Vadas, Yue and Becker, and graduate student)

Year 3:

• Same as year 2, but for the wintertime over the Rocky Mountains. Completion of the extraction and detailed analysis of ~ 100 estimated GOCE overpasses. Completion of the modeled secondary and tertiary GW spectra and comparison with GOCE GWs. (Drs. Vadas, Yue and Becker, and graduate student)

5. Intellectual Merit

Our proposed research explores the multi-step coupling of GWs from orographic forcing with the variability in the thermosphere via detailed data/modeling studies. This research will significantly advance our research community's knowledge of the transfer of momentum from orographic forcing to the thermosphere via GWs in this multi-step coupling process. This will lead to a much better understanding of the variability and structure of the thermosphere from these processes.

6. Expected Significance: Relevance to NSF and the Atmospheric Community

Observations show that the largest southern hemisphere wintertime GW hotspot at $z = 250 - 300$ km occurs over the Southern Andes, although the mechanism is currently unknown. Our proposed research would greatly increase our understanding of: 1) the detailed understanding of the process by which this hotspot is formed; 2) the amplitudes and scales of the GOCE GWs in the winter over the Southern Andes and Rocky Mountains; 3) the amplitudes and scales of the secondary and tertiary GWs at GOCE altitudes over the wintertime Southern Andes, Antarctic Peninsula and Rocky Mountains; and 4) the variability of the neutral wind in the thermosphere where the secondary GWs dissipate.

7. Broader Impacts

Because secondary GWs deposit momentum where they dissipate, these studies will lead to an enhanced understanding of the variability of the neutral winds in the winter thermosphere, and may help yield more-accurate calculations of satellite drag. To enhance scientific understanding to the research community and general public, this research will be disseminated via conference talks and journal publications. This project would also support the research of a graduate student and a woman scientist (PI). Our proposed research is thus highly relevant to the objectives of NSF, our community, and the general public.

8. Results from Prior NSF Support:

a. Sharon L. Vadas

Sharon has been/is a PI on two NSF grants within the past 5 years: (1) AGS-1139149 ($196,836, 03/01/12-02/28/15): "Collaborative Research: CEDAR–The Sources of gravity waves observed in the thermosphere at the Arecibo Observatory", and (2) AGS-1552315 ($355,366, 06/01/16-05/31/19): "Collaborative Research: CEDAR–Modeling and observation of secondary gravity waves in the thermosphere and ionosphere generated from deep convection". Highlights from this work include the derivation of the secondary GWs excited by horizontal and vertical body forces and heatings, modeling of the secondary GWs from mountain wave breaking and comparison with 630 nm airglow data, determination of the changes to the neutral wind and temperature in the thermosphere from the dissipation of GWs from deep convection worldwide, development of a GW excitation model from tsunamis and comparison with TEC observations, determination of the scales and amplitudes of the secondary GWs over the Southern Andes and McMurdo from the KMCM, and extraction of fishbone structures from lidar data at McMurdo. Twelve publications and 2 papers under review cite these grants, and are listed in the reference section of this proposal.

b. Jia Yue and Erich Becker

Drs. Yue and Becker have not been PIs on NSF grants.

References

Alexander, M. J., and H. Teitelbaum (2007), Observation and analysis of a large amplitude mountain wave event over the Antarctic peninsula, *J. Geophys. Res.*, *112*, D21103, doi:10.1029/2006JD008368.

Alexander, M. J., and H. Teitelbaum (2011), Three-dimensional properties of Andes mountain waves observed by satellite: A case study, *J. Geophys. Res.*, *116*, D23110, doi:10.1029/2011JD016151.

Alexander, M. J., et al. (2008), Global estimates of gravity wave momentum flux from High Resolution Dynamics Limb Sounder Observations, *J. Geophys. Res.*, *113 (D15S18)*, doi:10.1029/2010JD008807.

Azeem, I., S. L. Vadas, G. Crowley, andJ . J. Makela (2017), Traveling ionospheric disturbances over the United States induced by gravity waves from the 2011 Tohoku tsunami and comparison with gravity wave dissipative theory, *J. Geophys. Res. Space Physics, 122*, doi:10.1002/2016JA023659.

Bacmeister, J.T. and M.R. Schoeberl (1989), Breakdown of vertically propagating two-dimensional gravity waves forced by orography, *J. Atmos. Sci.*, *46*, 2109–2134.

Becker, E. (2004), Direct heating rates associated with gravity wave saturation, *J. Atmos. Terr. Phys.*, *66*, 683–696.

Becker, E. (2009), Sensitivity of the upper mesosphere to the lorenz energy cycle of the troposphere, *J. Atmos. Sci.*, *66*, 647666, doi:10.1175/2008JAS2735.1.

Becker, E. (2012), Dynamical control of the middle atmosphere, *Space Sci Rev*, DOI 10.1007/s11214-011-9841-5.

Becker, E., R. Knöpfel, and F.-J. Lübken (2015), Dynamically induced hemispheric differences in the seasonal cycle of the summer polar mesopause, *J. Atmos. Solar Terres. Phys.*, *129*, 128-141, doi:10.1016/j.jastp.2015.04.014.

Becker, E. (2017), Mean-flow effects of thermal tides in the mesosphere and lower thermosphere, *J. Atmos. Sci.*, *74*, 2043–2063, DOI: 10.1175/JAS-D-16-0194.1.

Becker, E. and S.L. Vadas (2018), Secondary gravity waves in the winter mesosphere: Results from a high-resolution global circulation model, *J. Geophys. Res. Atmos*, *123*, https://doi.org/10.1002/2017JD027460

Bossert, K., et al. (2015), Momentum flux estimates accompanying multiscale gravity waves over Mount Cook, New Zealand, on 13 July 2014 during the DEEPWAVE campaign, *J. Geophys. Res.*, *120*, 9323-9337, doi:10.1002/2015JD023197.

Bossert K., C. G. Kruse, C. J. Heale, D. C. Fritts, B. P. Williams, J. B. Snively, P.-D. Pautet, and M. J. Taylor (2017), Secondary gravity wave generation over New Zealand during the DEEPWAVE campaign, *J. Geophys. Res. Atmos.*, *122*, 7834-7850, doi:10.1002/2016JD026079.

Bruinsma, S.L. and J.M. Forbes (2008), Medium to large-scale density variability as observed by CHAMP, *Space Weath.*, *6*. S08002, doi:10.1029/2008SW000411.

Bruinsma, S. (2013), Air density and wind retrieval using GOCE data, Validation Rep. European Space Agency (ESA) AO/1-6367/10/NL/AF. Available at https://earth.esa.int/web/guest/missions/esa-operational-missions/goce/goce-thermospheric-data.

Bruinsma, S. L., E. Doornbos, and B. R. Bowman (2014), Validation of GOCE densities and thermosphere model evaluation, *Adv. Space Res.*, *54*, 576-585, doi:10.1016/j.asr.2014.04.008.

Chen, C., X. Chu, A. J. McDonald, S.L. Vadas, Z. Yu, W. Fong and X. Lu (2013), Inertia-gravity waves in Antarctica: A case study using simultaneous lidar and radar measurements at McMurdo/Scott Base (77.8° S, 166.7° E), *J. Geophys. Res.*, *118*, 115, doi:10.1002/jgrd.50318.

Chen, C., X. Chu, J. Zhao, B. R. Roberts, Z. Yu, W. Fong, X. Lu, and J. A. Smith (2016), Lidar observations of persistent gravity waves with periods of 3-10h in the Antarctic middle and upper atmosphere at McMurdo (77.83°S, 166.67°E), *J. Geophys. Res. Space Physics*, *121*, 1483–1502, doi:10.1002/2015JA022127.

Chen, C., and X. Chu (2017), Two-dimensional Morlet wavelet transform and its application to wave recognition methodology of automatically extracting two-dimensional wave packets from lidar observations in Antarctica, *J. Atmos. Sol.-Terr. Phys.*, doi:10.1016/j.jastp.2016.10.016.

DelGenio, A. D., and G. Schubert (1979), Gravity wave propagation in a diffusively separated atmosphere with height-dependent collision frequencies, *J. Geophys. Res.*, *84*, 4371–4378.

de la Torre, A., and P. Alexander (2005), Gravity waves above Andes detected from GPS radio occultation temperature profiles: Mountain forcing?, *Geophys. Res. Lett.*, *32*, L17815, doi:10.1029/2005GL022959.

de Wit, R. J., D. Janches, D. C. Fritts, R. Stockwell, and L. Coy (2017), Unexpected climatological behavior of MLT gravity wave momentum flux in the lee of the southern Andes hotspot, *Geophys. Res. Lett.*, *4*, 1172–1191.

Djuth, F.T., M.P. Sulzer, J.H. Elder, and V. B. Wickwar (1997), High-resolution studies of atmosphere-ionosphere coupling at Arecibo Observatory, Puerto Rico, *Radio Sci.*,*32*, 2321–2344.

Djuth, F.T., M.P. Sulzer, S.A. Gonzales, J.D. Mathews, J.H. Elder, and R.L. Walterscheid (2004), A continuum of gravity waves in the Arecibo thermosphere? *Geophys. Res. Lett.*, *31*, L16801, 10.1029/2003GL019376.

Doornbos, E., P. Visser, G. Koppenwallner, and B. Fritsche (2013), Air density and wind retrieval using GOCE data, European Space Agency (ESA) AO/1-6367/10/NL/AF, Algorithm Theoretical Basis Document. Available at *https* : *//earth.esa.int/web/guest/missions/esa* − *operational* − *missions/goce/goce* − *thermospheric* − *data*.

Doornbos, E., S. L. Bruinsma, B. Fritsche, G. Koppenwallner, P. Visser, J. van den IJssel, and J. de Teixeira de Encarnacao (2014), Air density and wind retrieval using GOCE data, Final Rep. European Space Agency (ESA) contract 4000102847/NL/EL. Available at *https* : *//earth.esa.int/web/guest/missions/esa* − *operational* − *missions/goce/goce* − *thermospheric* − *data*.

Doornbos, E. (2016), Air density and wind retrieval using GOCE data, European Space Agency (ESA) AO/1-6367/10/NL/AF, Version 1.5 Data Set User Manual. Available at *https* : *//earth.esa.int/web/guest/missions/esa* − *operational* − *missions/goce/goce* − *thermospheric* − *data*.

Drob, D. P., J. T. Emmert, J. W. Meriwether, J. J. Makela, E. Doornbos, M. Conde, G. Hernandez, J. Noto, K. A. Zawdie, S. E. McDonald, et al. (2015), An update to the Horizontal Wind Model (HWM): The quiet time thermosphere, *Earth and Space Science*, *2*, 301319, doi:10.1002/2014EA000089.

Eckermann, S. and C. Marks (1996), An idealized ray model of gravity wave-tidal interactions, *J. Geophys. Res.*, *101*, D16, doi:10.1029/96JD01660.

Eckermann, S.D and P. Preusse (1999), Global Measurements of Stratospheric Mountain Waves from Space, *Science*, *286 (5444)*, 1534–1537, DOI: 10.1126/science.286.5444.1534.

Ern, M., P. Preusse, M. J. Alexander, and C. D. Warner (2004), Absolute values of gravity wave momentum flux derived from satellite data, *J. Geophys. Res.*, *109*, D20103, doi:10.1029/2004JD004752.

Ern, M., P. Preusse, J. C. Gille, C. L. Hepplewhite, M. G. Mlynczak, J. M. Russell III, and M. Riese (2011), Implications for atmospheric dynamics derived from global observations of gravity wave momentum flux in stratosphere and mesosphere, *J. Geophys. Res.*, *116*, D19107, doi:10.1029/2011JD015821.

Forbes, J. M., S. L. Bruinsma, E. Doornbos, and X. Zhang (2016), Gravity wave-induced variability of the middle thermosphere, *J. Geophys. Res.*, *121*, 6914-6923, doi:10.1002/2016JA022923.

Franke, P.M. and W.A. Robinson (1999), Nonlinear behavior in the propagation of atmospheric gravity waves *J. Atmos. Sci.*, *56*, 3010–3027.

Fritts, D.C., S. Arendt, and Ø. Andreassen (1998), Vorticity dynamics in a breaking internal gravity wave. Part 2. Vortex interactions and transition to turbulence, *J. Fluid Mech.*, *367*, 47-65.

Fritts, D. C., S. L. Vadas, and Y. Yamada (2002), An estimate of strong local body forcing and gravity wave radiation based on OH airglow and meteor radar observations' *Geophys. Res. Lett.*, *29(10)*, 10.1029/2001GL013753.

Fritts, D. C., and M. J. Alexander (2003), Gravity wave dynamics and effects in the middle atmosphere, *Rev. Geophys.*, *41*, 1003, doi:10.1029/2001RG000106.

Fritts, D.C., S.L. Vadas, K. Wan, and J.A. Werne (2006), Mean and variable forcing of the middle atmosphere by gravity waves, *J. Atmos. Solar Terres. Phys.*, *68*, 247–265.

Fritts, D.C., R.B. Smith, M.J. Taylor, J.D. Doyle, S.D. Eckermann, A. Drnbrack, M. Rapp, B.P. Williams, P. Pautet, K. Bossert, N.R. Criddle, C.A. Reynolds, P.A. Reinecke, M. Uddstrom, M.J. Revell, R. Turner, B. Kaifler, J.S. Wagner, T. Mixa, C.G. Kruse, A.D. Nugent, C.D. Watson, S. Gisinger, S.M. Smith, R.S. Lieberman, B. Laughman, J.J. Moore, W.O. Brown, J.A. Haggerty, A. Rockwell, G.J. Stossmeister, S.F. Williams, G. Hernandez, D.J. Murphy, A.R. Klekociuk, I.M. Reid, and J. Ma (2016), The deep propagating gravity wave experiment (DEEPWAVE): An Airborne and ground-based exploration of gravity wave propagation and effects from their sources throughout the lower and middle atmosphere, *Bull. Amer. Meteor. Soc.*, *97*, 425453, https://doi.org/10.1175/BAMS-D-14-00269.1

Gong, J., D.L. Wu, and S.D. Eckermann, (2012), Gravity wave variances and propagation derived from AIRS radiances, *Atmos. Chem. Phys.*, *12*, 1701–1720, doi:10.5194/acp-12-1701-2012.

Gossard, E. E., and W. H. Hooke (1975), *Waves in the atmosphere*, 456 pp., Elsevier Scientific Publishing Co.

Gross, S.H., C.A. Reber, and F.T. Huang (1984), Large-scale waves in the thermosphere observed by the AE-C satellite, *IEEE Trans. Geosc. Rem. Sens.*, *GE-22*, 340–352.

Heale, C. J., K. Bossert, J. B. Snively, D. C. Fritts, P.-D. Pautet, and M. J. Taylor (2017), Numerical modeling of a multiscale gravity wave event and its airglow signatures over Mount Cook, New Zealand, during the DEEPWAVE campaign, *J. Geophys. Res.*, *122*, 846-860, doi:10.1002/2016JD025700.

Hecht, J. H. (2004), Instability layers and airglow imaging, *Rev. Geophys.*, *RG1001*, doi:10.1029/2003RG000131.

Hedin, A.E. and H.G. Mayr (1987), Characteristics of wavelike fluctuations in Dynamics Explorer neutral composition data, *J. Geophys. Res.*, *92*, 11159-11172.

Hendricks, E. A., J. D. Doyle, S. D. Eckermann, and Q. J. anf P. A. Reinecke (2014), What is the source of the stratospheric gravity wave belt in austral winter, *J. Atmos. Sci.*, *71*, 1583–1592, doi:10.1175/JAS-D-13-0332.1.

Hickey, M. P. and K. D. Cole (1988), A Numerical model for gravity wave dissipation in the Thermosphere, *J. Atmos. Terres. Phys.*, *50*, 689–697.

Hoffmann, P., M.J. Alexander, (2009), Retrieval of stratospheric temperatures from Atmospheric Infrared Sounder Radiance measurements for gravity wave studies, *J. Geophys. Res.*, *114, D07105*, doi:10.1029/2008JD011241.

Hoffmann, P., E. Becker, W. Singer, M. Placke, (2010), Seasonal variation of mesospheric waves at northern middle and high latitudes, *J. Atmos. Sol. Terres. Phys.*, *72*, 1068–1079, doi:10.1016/j.jastp.2010.07.002.

Hoffmann, L., Xue, X., and Alexander, M. J. (2013), A global view of stratospheric gravity wave hotspots located with Atmospheric Infrared Sounder observations, *J. Geophys. Res.*, *118*, 416434.

Holton, J. R. (1992), An Introduction to Dynamic Meteorology, Academic Press, San Diego, CA, 507 pp.

Holton, J.R. and M.J. Alexander (1999), Gravity waves in the mesosphere generated by tropospheric convection, *Tellus*, *51A-B*, 45–58.

Huang, C.M., F.S. Kuo, H.Y. Lue, and C.H. Liu (1992), Numerical simulations of the saturated gravity wave spectra in the atmosphere, *J. Atmos. Terres. Phys.*, *54*, 129-142.

Innis, J.L., and M. Conde (2002), Characterization of acoustic-gravity waves in the upper thermosphere using Dynamics Explorer 2 Wind and Temperature Spectrometer (WATS) and Neutral Atmosphere Composition Spectrometer (NACS) data, *J. Geophys. Res.*, *107*, A12, 1418, doi:10.1029/2002JA009370.

Jiang, J. H., D. L. Wu, and S. D. Eckermann (2002), Upper Atmosphere Research Satellite (UARS) MLS observation of mountain waves over the Andes, *J. Geophys. Res.*, *107(D20)*, 8273, doi:10.1029/2002JD002091.

Larsen, M.F. (2002), Winds and shears in the mesosphere and lower thermosphere: Results from four decades of chemical release wind measurements, *J. Geophys. Res.*, *107*, (A8) 10.1029/2001JA000218.

Larsen, M.F., A.Z. Liu, R.L. Bishop, and J.H. Hecht (2003), TOMEX: A comparison of lidar and sounding rocket chemical tracer wind measurements, *Geophys. Res. Lett*, *30*, (7) 10.1029/2002GL015678.

LeLong, M.-P. and T.J. Dunkerton (1998), Inertia-gravity wave breaking in three dimensions. Part I: Convectively stable waves, *J. Atmos. Sci.*, *55*, 2473-2488.

Li, F., A. Z. Liu, G. R. Swenson, J. H. Hecht, and W. A. Robinson (2005), Observations of gravity wave breakdown into ripples associated with dynamical instabilities, *J. Geophys. Res.*, *110*, D09S11, doi:10.1029/2004JD004849.

Lindzen, R. S. (1981), Turbulence and Stress Owing to Gravity Wave and Tidal Breakdown, *J. Geophys. Res.*, *86(C10)*, 9707–9714.

Liu, H.-L., P.B. Hays, and R.G. Roble (1999), A numerical study of gravity wave breaking and impacts on turbulence and mean state, *J. Atmos. Sci.*, *56*, 2152-2177.

Liu, H., N. Pedatella, and K. Hocke (2017), Medium-scale gravitywave activity in the bottomside F region in tropical regions, *Geophys. Res. Lett.*, *44*, 7099-7105, doi:10.1002/2017GL073855.

Liu, X., J., Yue, J., Xu, R. R., Garcia, J. M., Russell, III, M., Mlynczak, D. L., Wu, and T., Nakamura (2017), Variations of global gravity waves derived from 14 years of SABER temperature observations, *J. Geophys. Res. Atmos.*, *122*, 6231-6249, doi:10.1002/2017JD026604.

Lu, X., X. Chu, H. Li, C. Chen,, J. A. Smith, and S. L. Vadas (2017), Statistical characterization of high-to-medium frequency mesoscale gravity waves by lidar-measured vertical winds and temperatures in the MLT, *J. Atmos. Solar Terres. Phys.*, *162*, 3-15, https://doi.org/10.1016/j.jastp.2016.10.009.

Lund, T. S., and D. C. Fritts (2012), Numerical simulation of gravity wave breaking in the lower thermosphere, *J. Geophys. Res.*, *117*, D21105, doi:10.1029/2012JD017536.

Mayr, H.G., I. Harris, F.A. Herrero, N.W. Spencer, F. Varosi, and W.D. Pesnell (1990), Thermospheric gravity waves: observations and interpretation using the transfer function model (TEM), *Space Sci. Rev.*,*54*, 297–375.

Miyoshi Y. and H. Fujiwara (2008), Gravity waves in the thermosphere simulated by a general circulation model, *J. Geophys. Res.*, *113*, D01101, doi:10.1029/2007JD008874.

Nakamura, T., A. Higashikawa, T. Tsuda, and Y. Matsushita (1999), Seasonal variations of gravity wave structures in OH airglow with a CCD imager at Shigaraki, *Earth Planets Space*, *51*, 897-906.

Nicolls, M. J., S. L. Vadas, J. W. Meriwether, M. G. Conde, and D. Hampton (2012), The phases and amplitudes of gravity waves propagating and dissipating in the thermosphere: Application to measurements over Alaska, *J. Geophys. Res.*, *117*, A05323, doi:10.1029/2012JA017542.

Nicolls, M.J., S.L. Vadas, N. Aponte and M. P. Sulzer (2014), Horizontal wave parameters of daytime thermospheric gravity waves and E-Region neutral winds over Puerto Rico, *J. Geophys. Res.*, *119*, 576–600, doi:10.1002/2013JA018988.

Oliver, W. L., Y. Otsuka, M. Sato, T. Takami, and S. Fukao (1997), A climatology of F region gravity wave propagation over the middle and upper atmosphere radar, *J. Geophys. Res.*, *102*, 14,499–14,512.

Pitteway, M.L.V. and Hines, C.O. (1963), The viscous damping of atmospheric gravity waves, *Can. J. Phys.*, *41*, 1935–1948.

Plougonven, R., A. Hertzog, and H. Teitelbaum (2008), Observations and simulations of a large-amplitude mountain wave breaking over the Antarctic Peninsula, *J. Geophys. Res.*, *113*, D16113, doi:10.1029/2007JD009739.

Prusa, J.M., P.K. Smolarkiewicz, R.R. Garcia (1996), Propagation and breaking at high altitudes of gravity waves excited by tropospheric forcing, *J. Atmos. Sci.*, *53*, 2186-2216.

Rong, P., J. Yue, J. Russell III, D. Siskind, C. Randall (2017), Universal power law of the gravity wave manifestation in the AIM CIPS polar mesospheric cloud images, *Atmos Chemistry Physics Discussion*, minor revision.

Sato, K., S. Tateno, S. Watanabe and Y. Kawatani (2012), Gravity wave characteristics in the southern hemisphere revealed by a high-resolution middle-atmosphere general circulation model, *J. Atmos. Sci.*, *69*, 1378–1396, doi:10.1175/JAS-D-11-0101.1.

Satomura, T. and K. Sato (1999), Secondary generation of gravity waves associated with the breaking of mountain waves, *J. Atmos. Sci.*, *56*, 3847-3858.

Smith, S. A., D.C. Fritts, and T.E. Vanzandt (1987), Evidence for a saturated spectrum of atmospheric gravity waves, *J. Atmos. Sci.*, *44*, 1404–1410.

Snively, J. B., and V. P. Pasko (2003), Breaking of thunderstorm-generated gravity waves as a source of short-period ducted waves at mesopause altitudes, *Geophys. Res. Lett.*, *30(24)*, 2254, doi:10.1029/2003GL018436.

Snively, J. B., and V. P. Pasko (2008), Excitation of ducted gravity waves in the lower thermosphere by tropospheric sources, *J. Geophys. Res.*, *113*, A06303, doi:10.1029/2007JA012693.

Taylor, M. J., and M. A. Hapgood (1990), On the origin of ripple-type wave structure in the OH nightglow emission, *Planet. Space Sci.*, *38*, '1421-1430.

Taylor, M. J., M. B. Bishop, and V. Taylor (1995), All-sky measurements of short period waves imaged in the OI (557.7nm), Na(589.2nm) and near infared OH and O_2(0,1) nightglow emissions during the ALOHA-93 campaign, *Geophys. Res. Lett.*, *22*, 2833-2836.

Tsuda, T., M. Nishida, C. Rocken, and R. H. Ware, (2000), A global morphology of gravity wave activity in the stratosphere revealed by the GPS occultation data (GPS/MET), *J. Geophys. Res.*, *105*, 7257–7273.

Vadas, S. L., and D. C. Fritts (2001), Gravity wave radiation and mean responses to local body forces in the atmosphere, *J. Atmos. Sci.*, *58*, 2249–2279.

Vadas, S. L., and D. C. Fritts (2002), The importance of spatial variability in the generation of secondary gravity waves from local body forces, *Geophys. Res. Lett.*, *29(20)*, doi:10.1029/2002GL015574.

Vadas, S. L., D. C. Fritts, and M.J. Alexander (2003), Mechanism for the generation of secondary waves in wave breaking regions, *J. Atmos. Sci.*, *60*, 194–214.

Vadas, S. L, and D. C. Fritts (2004), Thermospheric responses to gravity waves arising from mesoscale convective complexes, *J. Atmos. Solar Terres. Phys.*, *66*, 781–804.

Vadas, S. L., and D. C. Fritts (2005), Thermospheric responses to gravity waves: Influences of increasing viscosity and thermal diffusivity, *J. Geophys. Res.*, *110*, D15103, doi:10.1029/2004JD005574.

Vadas, S. L., and D. C. Fritts (2006), Influence of solar variability on gravity wave structure and dissipation in the thermosphere from tropospheric convection, *J. Geophys. Res.*, *111*, A10S12, doi:10.1029/2005JA011510.

Vadas, S. L. (2007), Horizontal and vertical propagation and dissipation of gravity waves in the thermosphere from lower atmospheric and thermospheric sources, *J. Geophys. Res.*, *112*, A06305, doi:10.1029/2006JA011845.

Vadas, S. L., and D. C. Fritts (2009), Reconstruction of the gravity wave field from convective plumes via ray tracing, *Ann. Geophys.*, *27*, 147–177.

Vadas, S. L. and H.-L. Liu (2009), The generation of large-scale gravity waves and neutral winds in the thermosphere from the dissipation of convectively-generated gravity waves, *J. Geophys. Res.*, *114*, A10310, doi:10.1029/2009JA014108.

Vadas, S. L., M. J. Taylor, P.-D. Pautet, P. A. Stamus, D. C. Fritts, H.-L. Liu, F. T. Sao Sabbas, V. T. Rampinelli, P. Batista and H. Takahashi (2009a), Convection: the likely source of medium-scale gravity waves observed in the OH airglow layer near Basilia, Brazil, during the SpreadFEx Campaign, *Ann. Geophys.*, *27*, 231–259.

Vadas, S. L., J. Yue, C.-Y. She, P.A. Stamus and A. Liu (2009b), A model study of the effects of winds on concentric rings of gravity waves from a convective plume near Fort Collins on 11 May 2004, *J. Geophys. Res.*, *114*, D06103, doi:10.1029/2008JD010753.

Vadas, S.L. and G. Crowley (2010), Sources of the traveling ionospheric disturbances observed by the ionospheric TIDDBIT sounder near Wallops Island on October 30, 2007, *J. Geophys. Res.*, *115*, A07324, doi:10.1029/2009JA015053.

Vadas, S.L. and M.J. Nicolls (2012), The phases and amplitudes of gravity waves propagating and dissipating in the thermosphere: Theory, *J. Geophys. Res.*, *117*, A05322, doi:10.1029/2011JA017426.

Vadas, S.L., J. Yue, and T. Nakamura (2012), Mesospheric concentric gravity waves generated by multiple convection storms over the North America Great Plain, *J. Geophys. Res.*, *117*, D7, doi:10.1029/2011JD017025.

Vadas, S. L., and H.-L. Liu (2013), Numerical modeling of the large-scale neutral and plasma responses to the body forces created by the dissipation of gravity waves from 6 h of deep convection in Brazil, *J. Geophys. Res.*, *118*, 2593–2617, doi:10.1002/jgra.50249.

Vadas, S. L. (2013), Compressible f-plane solutions to body forces, heatings, and coolings, and application to the primary and secondary gravity waves generated by a deep convective plume, *J. Geophys. Res.*, *118*, 2377–2397, doi:10.1002/jgra.50163.

Vadas, S. L., and D. C. Fritts (2013), Corrigendum, *J. Atmos. Sci.*, *70*, DOI: 10.1175/JAS-D-13-057.1, 2680.

Vadas, S.L., H.-L. Liu, and R.S. Lieberman (2014), Numerical modeling of the global changes to the thermosphere and ionosphere from the dissipation of gravity waves from deep convection *J. Geophys. Res.*, *119*, 7762–7793, doi:10.1002/2014JA020280.

Vadas, S. L., J. J. Makela, M. J. Nicolls, and R. F. Milliff (2015), Excitation of gravity waves by ocean surface wave packets: Upward propagation and reconstruction of the thermospheric gravity wave field, *J. Geophys. Res.*, *120*, doi:10.1002/2015JA021430.

Vadas, S.L. and G. Crowley (2017), Neutral wind and density perturbations in the thermosphere created by gravity waves observed by the TIDDBIT sounder, *J. Geophys. Res. Space Physics*, *122*, 66526678, doi:10.1002/2016JA023828.

Vadas, S.L. and E. Becker (2017), The Excitation, Propagation, and Dissipation of Primary and Secondary Gravity Waves from during Wintertime in Antarctica, *J. Geophys. Res. Atmos.*, under review, available at https : //www.cora.nwra.com/ $\sim$ vasha/VadasBecker2017.pdf.

Vadas, S.L., J. Zhao, X. Chu and E. Becker (2017), The Excitation of Medium to Large-Scale Secondary Gravity Waves from Body Forces: Theory and Observation, *J. Geophys. Res. Atmos.*, under review, available at https : //www.cora.nwra.com/ $\sim$ vasha/Vadasetal_2017.pdf.

Vincent, R.A., A. Hertzog, G. Boccara and F. Vial (2007), Quasi-Lagrangian superpressure balloon measurements of gravity-wave momentum fluxes in the polar stratosphere of both hemispheres, *Geophys. Res. Lett.*, *34*, L19804, doi:10.1029/2007GL031072.

Volland, H. (1969), Full wave calculations of gravity wave propagation through the thermosphere, *J. Geophys. Res.*, *74*,1786–1795.

Walterscheid, R.L. and G. Schubert (1990), Nonlinear evolution of an upward propagating gravity wave: overturning, convection, transcience and turbulence, *J. Atmos. Sci.*, *47*, 101-125.

Walterscheid, R.L., L.J. Gelinas, C.R. Mechoso, and G. Schubert (2016), Spectral distribution of gravity wave momentum fluxes over the Antarctic Peninsula from Concordiasi superpressure balloon data, *J. Geophys. Res. Atmos.*, *121*, 7509–7527, doi:10.1002/2015JD024253.

Watanabe, S., K. Sato, and M. Takahashi (2006), A general circulation model study of orographic gravity waves over Antarctica excited by katabatic winds, *J. Geophys. Res.*, *111*, D18104, doi:10.1029/2005JD006851.

Wu, D. L., and J. H. Jiang (2002), MLS observations of atmospheric gravity waves over Antarctica, *J. Geophys. Res.*, *107 (D24)*, 4773, doi:10.1029/2002JD002390.

Wu, D.L., P. Preusse, S.D. Eckermann, J.H. Jiang, M. de la T. Juarez, L. Coy, and D. Y. Wang (2006), Remote sounding of atmospheric gravity waves with satellite limb and nadir techniques, *Advances in Space Research*, *37*, 22692277, doi:10.1016/j.asr.2005.07.031.

Yamada, Y., H. Fukunishi, T. Nakamura, and T. Tsuda (2001), Breaking of small-scale gravity wave and transition to turbulence observed in OH airglow, *Geophys. Res. Lett.*, *28*, 2153–2156.

Yiğit, E., A.D. Aylward and A.S. Medvedev (2008), Parameterization of the effects of vertically propagating gravity waves for thermosphere general circulation models: Sensitivity study, *J. Geophys. Res.*, *113*, D19106, doi:10.1029/2008JD010135.

Yiğit, E., A.S. Medvedev, A.D. Aylward, P. Hartogh, M.J. Harris (2009), Modeling the effects of gravity wave momentum deposition on the general circulation above the turbopause, *J. Geophys. Res.*, *114*, D07101, doi:10.1029/2008JD011132.

Yue J., L. Hoffmann, and M.J. Alexander (2013), Simultaneous observations of convective gravity waves from a ground-based airglow imager and the AIRS satellite experiment, *J. Geophys. Res.*, *118*, 3178-3191, doi:10.1002/jgrd.50341.

Yue, J., B. Thurairajah, L. Hoffmann, M. J. Alexander, A. Chandran, M. J. Taylor, J. M. Russell III, C. E. Randall, and S. M. Bailey (2014a), Concentric gravity waves in polar mesosphere clouds from the Cloud Imaging and Particle Size experiment, *J. Geophys. Res.*, *119*, 5115-5127, doi:10.1002/2013JD021385.

Yue, J., S. Miller, L. Hoffmann, and W. C. Straka III (2014b), Stratospheric and mesospheric concentric gravity waves over tropical cyclone Mahasen: Joint AIRS and VIIRS satellite observations, *J. Atmos. Solar Terres. Phys.*, *119*, 83-90, doi:10.1016/j.jastp.2014.07.003.

Zhao, J., X. Chu, C. Chen, X. Lu, W. Fong, Z. Yu, R. M. Jones, B.R. Roberts, and Andreas Dörnbrack (2017), Lidar observations of stratospheric gravity waves from 2011 to 2015 at McMurdo (77.84° S, 166.69° E), Antarctica: Part I. Vertical wavelengths, periods, and frequency and vertical wavenumber spectra, *J. Geophys. Res.*, *122*, doi:10.1002/2016JD026368.

Vadas References for Results from Prior NSF Support

Chen, C., X. Chu, A. J. McDonald, S. L. Vadas, Z. Yu, W. Fong, and X. Lu (2013), Inertia-gravity waves in Antarctica: A case study using simultaneous lidar and radar measurements at McMurdo/Scott Base (77.8° S, 166.7° E). *J. Geophys. Res*, **118**, 115, doi:10.1002/jgrd.50318.

Liu, X., J. Xu, J. Yue and S. L. Vadas (2013), Numerical modeling study of the momentum deposition of small amplitude gravity waves in the thermosphere. *Ann. Geophys.*, **31**, 1-14.

Smith, S. M., S. L. Vadas, W. J. Baggaley, G. Hernandez, and J. Baumgardner (2013), Gravity wave coupling between the mesosphere and thermosphere over New Zealand. *J. Geophys. Res. Space Physics*, **118**, 26942707, doi:10.1002/jgra.50263.

Suzuki, H., T. Nakamura, S. L. Vadas, M. Tsutsumi, and M. Taguchi (2013), Inertia-gravity wave in the polar mesopause region inferred from successive images of a meteor train, *J. Geophys. Res. Atmos.*, **118**, 30473052, doi:10.1002/jgrd.50228.

Suzuki, S., S. L. Vadas, K. Shiokawa, Y. Otsuka, S. Kawamura, and Y. Murayama (2013), Typhoon-induced concentric airglow structures in the mesopause region. Geophys. Res. Lett., **40**, 59835987, doi:10.1002/2013GL058087.

Vadas, S. L. (2013), Compressible f-plane solutions to body forces, heatings, and coolings, and application to the primary and secondary gravity waves generated by a deep convective plume. *J. Geophys. Res. Space Physics*, **118**, 23772397, doi:10.1002/jgra.50163.

Nicolls, M. J., S. L. Vadas, N. Aponte, and M. P. Sulzer (2014), Horizontal wave parameters of daytime thermospheric gravity waves and E-region neutral winds over Puerto Rico. *J. Geophys. Res. Space Physics*, **119**, 575600, doi:10.1002/2013JA018988.

Vadas, S. L., H. Suzuki, M. J. Nicolls, T. Nakamura and R.O. Harmon (2014), Atmospheric gravity waves excited by a fireball meteor: Observations and modeling, *J. Geophys. Res. Space Physics*, **119**, doi:10.1002/2014JD021664.

Vadas, S. L., J. J. Makela, M. J. Nicolls, and R. F. Milliff (2015), Excitation of gravity waves by ocean surface wave packets: Upward propagation and reconstruction of the thermospheric gravity wave field. *J. Geophys. Res. Space Physics*, **120**, 97489780, doi:10.1002/2015JA021430.

Azeem, I., S. L. Vadas, G. Crowley, and J. J. Makela (2017), Traveling ionospheric disturbances over the United States induced by gravity waves from the 2011 Tohoku tsunami and comparison with gravity wave dissipative theory. *J. Geophys. Res. Space Physics,* **122**, 34303447, doi:10.1002/2016JA023659.

Vadas, S. L. and G. Crowley (2017), Neutral wind and density perturbations in the thermosphere created by gravity waves observed by the TIDDBIT sounder. J. Geophys. Res. Space Physics, **122**, 66526678, doi:10.1002/2016JA023828.

Becker, E. and S. L. Vadas (2018), "Secondary gravity waves in the winter mesosphere: Results from a high-resolution global circulation model", *J. Geophys. Res. Atmospheres*, **123**, https://doi.org/10.1002/2017JD027460.

Vadas, S.L. and E. Becker, The Excitation, Propagation, and Dissipation of Primary and Secondary Gravity Waves from during Wintertime in Antarctica, *J. Geophys. Res. Atmos.*, under review, available at https : //www.cora.nwra.com/ $\sim$ vasha/VadasBecker2017.pdf.

Vadas, S.L., J. Zhao, X. Chu and E. Becker, The Excitation of Medium to Large-Scale Secondary Gravity Waves from Body Forces: Theory and Observation, *J. Geophys. Res. Atmos.*, under review, available at https : //www.cora.nwra.com/ $\sim$ vasha/Vadasetal_2017.pdf.

Biographical Sketch for Sharon L. Vadas

ADDRESS: NorthWest Research Associates, CoRA Office
3380 Mitchell Lane, Boulder, CO 80301, USA

Professional Preparation:

B.A. Physics & Chemistry	Univ. of Rochester	1987
M.A. Physics	Univ. of Chicago	1990
Ph.D. Physics	Univ. of Chicago	1993

Appointments:

2010-present	Senior Research Scientist	NWRA, CoRA Office
1997-2010	Research Scientist	NWRA, CoRA Office
1995-1997	Postdoctoral Fellow	LASP, Univ of Colorado, Boulder
1993-1995	President's Postdoctoral Fellow	Univ. of California, Berkeley
1993	Guest Scientist	Fermi National Accelerator Lab

5 Most Relevant Products:

Vadas, S. L. and M. J. Nicolls, 2012, "The Phases and amplitudes of gravity waves propagating and dissipating in the thermosphere: Theory", *J. Geophys. Res,* **117**, A05322, doi:10.1029/2011JA017426.

Becker, E. and S.L. Vadas, 2018, "Secondary gravity waves in the winter mesosphere: Results from a high-resolution global circulation model", *J. Geophys. Res. Atmospheres,* doi:10.1002/2017JD027460, in press.

Vadas, S.L., D.C. Fritts, and M.J. Alexander, 2003: "Mechanism for the generation of secondary waves in wave breaking regions", *J. Atmos. Sci.*, **60**, 194–214.

Vadas, S.L. and D.C. Fritts, 2002: "The Importance of spatial variability in the generation of secondary gravity waves from local body forces", *Geophys. Res. Lett*., **29**(20) 10.1029/2002GL015574.

Vadas, S. L., 2013, "Compressible f-plane solutions to body forces, heatings, and coolings, and application to the primary and secondary gravity waves generated by a deep convective plume", *J. Geophys. Res.*, 118, 2377-2397, doi:10.1002/jgra.50163.

5 Other Relevant Products:

Vadas, S.L. and D.C. Fritts, 2005: "Thermospheric responses to gravity waves: Influences of increasing viscosity and thermal diffusivity" *J. Geoph. Res*., **110**, D15103; doi:10.1029/2004JD005574.

Vadas, S.L., J. Yue, and T. Nakamura, 2012, ``Mesospheric concentric gravity waves generated by multiple convection storms over the North America Great Plain", *J. Geophys. Res*, **117**, D7, doi:10.1029/2011JD017025.

Vadas, S. L., and M. J. Nicolls, 2009: "Temporal evolution of neutral, thermospheric winds and plasma response using PFISR measurements of gravity waves"', *J. Atmos. Solar Terres. Phys*., **71**, 740-770.

Vadas, S.L., J. Yue, C.-Y. She, P.A. Stamus, and A.Z. Liu, 2009: "A model study of the effects of winds on concentric rings of gravity waves from a convective plume near Fort Collins on 11 May 2004", *J. Geoph. Res.,* **114**, D06103, doi:10.1029/2008JD010753.

Vadas, S.L., H.-L. Liu, and R.S. Lieberman, 2014, "Numerical modeling of the global changes to the thermosphere and ionosphere from the dissipation of gravity waves from deep convection", *J. Geophys. Res. Space Physics*, **119**, doi:10.1002/2014JA020280.

Synergistic Activities:

- Derived the 3D Boussinesq and compressible, f-plane solutions for temporally and spatially varying heatings and body forcings, and implemented them into a fortran-90 code. Developed models for the excitation of (larger-scale) secondary GWs from stratospheric, mesospheric, and thermospheric body forces; these secondary GWs have larger horizontal wavelengths and phase speeds than those of the primary GWs, and can therefore typically propagate to much higher altitudes than the primary GWs. Developed models for the excitation of GWs from deep convective plumes.
- Used the secondary GW theory to identify several "fishbone" structures in the MLT in Dr. Xinzhao Chu's lidar data at McMurdo Station in the Antarctica. Fishbone structures signal the presence of secondary GWs excited by body forces created from the dissipation of primary GWs. Submitted a paper on this topic to *J. Geophys. Res. Atmospheres:* Vadas, S.L., J. Zhao, X. Chu and E. Becker, "The Excitation of secondary gravity waves from body forces: Theory and observation" (under review. submitted 10/17, revised 2/18).
- Analyzed the wintertime primary and larger-scale secondary GWs over McMurdo using the model data from the Kuelungsborn Mechanistic general Circulation Model (KMCM). Created a novel technique which transforms the data to equally-spaced horizontal grids; this allows for the straightforward determination of the GW characteristics near the pole. Showed that the dissipation of katabatic mountain waves (MWs) over McMurdo creates body forces that excite larger-scale secondary GWs which propagate to the MLT, and that most of the GWs above 70 km altitude are secondary GWs. Submitted a paper on this topic to *J. Geophys. Res. Atmospheres*: Vadas, S.L. and E. Becker, "The Excitation, propagation, and dissipation of primary and secondary gravity waves during wintertime at McMurdo Station in the Antarctic" (under review. submitted 10/17, minor revisions, revised 2/18).
- Derived a more complete 3D gravity wave (GW) anelastic, dissipative dispersion relation which includes kinematic viscosity and thermal diffusivity in the thermosphere, and implemented it into a fortran-90 3D ray trace code. Using reverse ray-tracing, determined the sources of gravity waves 1) observed in the OH layer in Brazil and in Colorado, 2) observed by PFISR/Alaska in the ionosphere, and 3) observed by TIDDBIT at the bottomside of the F layer in Virginia. Wind and temperature models were built from balloon soundings, the TIME-GCM, ECMWF, and/or MSIS. Using forward ray-tracing, determined the GW and OH airglow perturbations created bv GWs excited by deep convective plumes, clusters, and complexes, and tsunamis.
- Used the GW dissipative polarization and dispersion relations to determine the intrinsic frequency, horizontal and vertical wavlengths, and propagation directions of GWs observed by a satellite measuring the in-situ cross-track wind and density. Used this technique to determine these GW quantitides in the MLT with a lidar and in the thermosphere with a Fabry-Perot Interferometer. Extracted the neutral, thermospheric winds from altitudinal profiles of GW vertical wavelengths using PFISR electron densities and the GW dissipative dispersion relation.

Graduate Thesis Advisor:

E. W. Kolb U. Chicago

Postdoctoral Advistors:

Josesph Silk U. of Oxford

Biographical Sketch
Erich Becker

Address: Leibniz Institute of Atmospheric Physics
at the University of Rostock e.V. (IAP),
Schlossstr. 6, 18226 Kühlungsborn, Germany

Professional preparation

1988	Diploma[1)] in Physics	University of Marburg, Germany
1991	Ph.D. in Physics	University of Göttingen, Germany
2003	Habilitation[2)] in Physics	University of Rostock, Germany

1) equivalent to M.S.
2) traditional degree required in Germany to obtain a faculty position

Appointments

2006-present	Head of Dep. of Theory & Modeling	IAP
2006-present	Professor of Atmospheric Physics	University of Rostock, Germany
1993-2006	Senior Scientist	IAP
1991-1993	Postdoctoral Fellow	Max Planck Institute of Fluid Mechanics, Göttingen, Germany

5 most relevant publications

Becker, E, 2017. Mean-flow effects of thermal tides in the mesosphere and lower thermosphere. *J. Atmos. Sci.*, **76**, 2043-2063, doi:10.1175/JAS-D-16-0194.1.

Becker, E., 2012. Dynamical control of the middle atmosphere. *Space Sci. Rev.*, doi:10.1007/s11214-011-9841-5.

Becker, E., 2009. Sensitivity of the upper mesosphere to the Lorenz energy cycle of the troposphere. *J. Atmos. Sci.*, **66**, 647-666.

Becker, E. and C. McLandress, 2009. Consistent scale interaction of gravity waves in the Doppler-spread parameterization. *J. Atmos. Sci.*, **66**, 1434-1449.

Becker, E. and D. C. Fritts, 2006. Enhanced gravity-wave activity and interhemispheric coupling during the MaCWAVE/MIDAS northern summer program 2002. *Ann. Geophys.*, **24**, 1175-1188.

Other 5 relevant publications

Karlsson, B. and E. Becker, 2016. How does interhemispheric coupling contribute to cool down the summer polar mesosphere? *J. Clim.*, **29**, 8807-8821, doi:10.1175/JCLI-D-16-0231.1.

Becker, E., R. Knöpfel, and F.-J. Lübken, 2015. Dynamically induced hemispheric differences in the seasonal cycle of the summer polar mesopause. *J. Atmos. Sol.-Terr. Phys.*, **129**, 128-141.

Brune, S. and E. Becker, 2013. Indications of stratified turbulence in a mechanistic GCM. *J. Atmos. Sci.*, **70**, 231-247, doi:10.1175/JAS-D-12-025.1.

Becker, E. and C. v. Savigny, 2010. Dynamical heating of the polar summer mesopause induced by solar proton events. *J. Geophys. Res.*, doi:10.1029/2009JD012561.

Hoffmann, P., E. Becker, W. Singer, and M. Placke, 2010. Seasonal variation of mesospheric waves at middle and high latitudes. *J. Atmos. Sol.-Terr. Phys.*, **72**, 1068-1079.

Synergistic activities

- Developed the *Kühlungsborn Mechanistic general Circulation Model (KMCM)*. The latest version includes all components of a climate model (radiation, moisture cycle, simple ocean model) and extends up to z∼200 km. Developed a new *GW-resolving version* of the KMCM by combining high resolution with a *hydrodynamically consistent subgrid-scale parameterization* based on the nonlinear Smagorinsky model for horizontal and vertical diffusion.
- Used the GW-resolving KMCM for the following investigations: 1) Showed that the intermittent body forces due to primary orographic GWs in the southern winter stratopause region give rise to *secondary GWs* that play a vital role in the southern winter mesopause region; 2) showed that these secondary GWs explain the amplitudes, periods, and vertical wavenumbers seen in lidar temperature measurements over McMurdo during wintertime at z∼80-100 km; 3) showed that secondary GWs in the polar winter upper mesosphere are required to simulate realistic mean zonal winds; 4) showed that GW amplitudes in the summer mesosphere scale with the intensity of the (tropospheric) Lorenz energy cycle; 5) showed that the annual and semi-annual variations of GW activity in the upper mesosphere as observed in the northern hemisphere by radars result from wind-induced GW dissipation; 6) showed that solar proton events can lead to temporary heating of the summer polar mesopause due to modulation of GW dissipation.
- Developed theory for the *energy deposition* of parameterized gravity waves (GWs) and resolved waves in general circulation models. Applied the theory to interpret measurements of the turbulent dissipation rate in the mesosphere, including its summer-winter asymmetry. Estimated the role of thermal tides in the zonal-mean momentum and sensible heat budgets of the lower thermosphere.
- Analyzed the role of planetary Rossby waves forced in the troposphere for the residual circulation in the mesosphere/lower thermosphere (MLT). Discovered the *Interhemispheric Coupling* mechanism and applied it to measurements. Analyzed *hemispheric differences* in the seasonal cycle of the summer polar mesopause and interpreted measurements at the sites of Davis (Antarctica) and Andenes (Norway).
- Performed the first simulation of the Lorenz energy cycle with the correct generation of unavailable potential energy. Simulated the Nastrom-Gage spectrum in the troposphere using the KMCM with very high resolution, analyzed the macro-turbulent kinetic budget and showed that the concept of *stratified turbulence* applies to the mesoscales.

Teaching and and supervision of students

- Taught two graduate courses per year since 2007 as part of the Physics Master Program at the University of Rostock: *Dynamics of the Atmosphere* and *Physics of Climate*.
- Gave general lectures on Atmospheric Physics during international summer schools at IAP in 2012, 2013, 2014, and 2016.
- Supervised 6 diploma/master graduate students (all finished) and 8 PhD graduate students (3 finished, 5 are currently working on their theses) at IAP. Supervised several undergraduate students.

Advisors

Diploma	U. Brosa, S. Großmann	University of Marburg, Germany
PhD thesis	F. Obermeier, E. A. Müller	Max Planck Institute of Fluid Mechanics, Göttingen, Germany

SUMMARY PROPOSAL BUDGET

YEAR 1

FOR NSF USE ONLY		
PROPOSAL NO.	DURATION (months) Proposed	Granted
AWARD NO.		

ORGANIZATION
NorthWest Research Associates, Incorporated

PRINCIPAL INVESTIGATOR / PROJECT DIRECTOR
Sharon L Vadas

A. SENIOR PERSONNEL: PI/PD, Co-PI's, Faculty and Other Senior Associates (List each separately with title, A.7. show number in brackets)	NSF Funded Person-months CAL	ACAD	SUMR	Funds Requested By proposer	Funds granted by NSF (if different)
1. **Sharon L Vadas - PI**	4.30	0.00	0.00	**49,589**	
2. **Erich Becker - Co-PI**	0.50	0.00	0.00	**5,237**	
3.					
4.					
5.					
6. (**0**) OTHERS (LIST INDIVIDUALLY ON BUDGET JUSTIFICATION PAGE)	0.00	0.00	0.00	**0**	
7. (**2**) TOTAL SENIOR PERSONNEL (1 - 6)	4.80	0.00	0.00	**54,826**	
B. OTHER PERSONNEL (SHOW NUMBERS IN BRACKETS)					
1. (**0**) POST DOCTORAL SCHOLARS	0.00	0.00	0.00	**0**	
2. (**0**) OTHER PROFESSIONALS (TECHNICIAN, PROGRAMMER, ETC.)	0.00	0.00	0.00	**0**	
3. (**0**) GRADUATE STUDENTS				**0**	
4. (**0**) UNDERGRADUATE STUDENTS				**0**	
5. (**0**) SECRETARIAL - CLERICAL (IF CHARGED DIRECTLY)				**0**	
6. (**0**) OTHER				**0**	
TOTAL SALARIES AND WAGES (A + B)				**54,826**	
C. FRINGE BENEFITS (IF CHARGED AS DIRECT COSTS)				**17,599**	
TOTAL SALARIES, WAGES AND FRINGE BENEFITS (A + B + C)				**72,425**	
D. EQUIPMENT (LIST ITEM AND DOLLAR AMOUNT FOR EACH ITEM EXCEEDING $5,000.)					
TOTAL EQUIPMENT				**0**	
E. TRAVEL 1. DOMESTIC (INCL. U.S. POSSESSIONS)				**3,180**	
2. INTERNATIONAL				**0**	
F. PARTICIPANT SUPPORT COSTS					
1. STIPENDS $ **0**					
2. TRAVEL **0**					
3. SUBSISTENCE **0**					
4. OTHER **0**					
TOTAL NUMBER OF PARTICIPANTS (**0**) TOTAL PARTICIPANT COSTS				**0**	
G. OTHER DIRECT COSTS					
1. MATERIALS AND SUPPLIES				**0**	
2. PUBLICATION COSTS/DOCUMENTATION/DISSEMINATION				**4,060**	
3. CONSULTANT SERVICES				**0**	
4. COMPUTER SERVICES				**1,173**	
5. SUBAWARDS				**0**	
6. OTHER				**0**	
TOTAL OTHER DIRECT COSTS				**5,233**	
H. TOTAL DIRECT COSTS (A THROUGH G)				**80,838**	
I. INDIRECT COSTS (F&A)(SPECIFY RATE AND BASE) **General and Administrative (Rate: 16.0000, Base: 111981) (Cont. on Comments Page)**					
TOTAL INDIRECT COSTS (F&A)				**49,060**	
J. TOTAL DIRECT AND INDIRECT COSTS (H + I)				**129,898**	
K. SMALL BUSINESS FEE				**0**	
L. AMOUNT OF THIS REQUEST (J) OR (J MINUS K)				**129,898**	

M. COST SHARING PROPOSED LEVEL $ **0** AGREED LEVEL IF DIFFERENT $

PI/PD NAME
Sharon L Vadas

ORG. REP. NAME*

FOR NSF USE ONLY		
INDIRECT COST RATE VERIFICATION		
Date Checked	Date Of Rate Sheet	Initials - ORG

 ***ELECTRONIC SIGNATURES REQUIRED FOR REVISED BUDGET**

SUMMARY PROPOSAL BUDGET COMMENTS - Year 1

**** I- Indirect Costs**
Overhead (Rate: 43.0000, Base 72425)

SUMMARY PROPOSAL BUDGET

YEAR 2

FOR NSF USE ONLY		
PROPOSAL NO.	DURATION (months) Proposed	Granted
AWARD NO.		

ORGANIZATION
NorthWest Research Associates, Incorporated

PRINCIPAL INVESTIGATOR / PROJECT DIRECTOR
Sharon L Vadas

A. SENIOR PERSONNEL: PI/PD, Co-PI's, Faculty and Other Senior Associates (List each separately with title, A.7. show number in brackets)	NSF Funded Person-months CAL	ACAD	SUMR	Funds Requested By proposer	Funds granted by NSF (if different)
1. **Sharon L Vadas - PI**	4.20	0.00	0.00	**49,472**	
2. **Erich Becker - Co-PI**	0.50	0.00	0.00	**5,363**	
3.					
4.					
5.					
6. (**0**) OTHERS (LIST INDIVIDUALLY ON BUDGET JUSTIFICATION PAGE)	0.00	0.00	0.00	**0**	
7. (**2**) TOTAL SENIOR PERSONNEL (1 - 6)	4.70	0.00	0.00	**54,835**	
B. OTHER PERSONNEL (SHOW NUMBERS IN BRACKETS)					
1. (**0**) POST DOCTORAL SCHOLARS	0.00	0.00	0.00	**0**	
2. (**0**) OTHER PROFESSIONALS (TECHNICIAN, PROGRAMMER, ETC.)	0.00	0.00	0.00	**0**	
3. (**0**) GRADUATE STUDENTS				**0**	
4. (**0**) UNDERGRADUATE STUDENTS				**0**	
5. (**0**) SECRETARIAL - CLERICAL (IF CHARGED DIRECTLY)				**0**	
6. (**0**) OTHER				**0**	
TOTAL SALARIES AND WAGES (A + B)				**54,835**	
C. FRINGE BENEFITS (IF CHARGED AS DIRECT COSTS)				**17,602**	
TOTAL SALARIES, WAGES AND FRINGE BENEFITS (A + B + C)				**72,437**	
D. EQUIPMENT (LIST ITEM AND DOLLAR AMOUNT FOR EACH ITEM EXCEEDING $5,000.)					
TOTAL EQUIPMENT				**0**	
E. TRAVEL 1. DOMESTIC (INCL. U.S. POSSESSIONS)				**3,180**	
2. INTERNATIONAL				**0**	
F. PARTICIPANT SUPPORT COSTS					
1. STIPENDS $ **0**					
2. TRAVEL **0**					
3. SUBSISTENCE **0**					
4. OTHER **0**					
TOTAL NUMBER OF PARTICIPANTS (**0**) TOTAL PARTICIPANT COSTS				**0**	
G. OTHER DIRECT COSTS					
1. MATERIALS AND SUPPLIES				**0**	
2. PUBLICATION COSTS/DOCUMENTATION/DISSEMINATION				**4,060**	
3. CONSULTANT SERVICES				**0**	
4. COMPUTER SERVICES				**1,146**	
5. SUBAWARDS				**0**	
6. OTHER				**0**	
TOTAL OTHER DIRECT COSTS				**5,206**	
H. TOTAL DIRECT COSTS (A THROUGH G)				**80,823**	
I. INDIRECT COSTS (F&A)(SPECIFY RATE AND BASE) **General and Administrative (Rate: 16.0000, Base: 111971) (Cont. on Comments Page)**					
TOTAL INDIRECT COSTS (F&A)				**49,063**	
J. TOTAL DIRECT AND INDIRECT COSTS (H + I)				**129,886**	
K. SMALL BUSINESS FEE				**0**	
L. AMOUNT OF THIS REQUEST (J) OR (J MINUS K)				**129,886**	

M. COST SHARING PROPOSED LEVEL $ **0** AGREED LEVEL IF DIFFERENT $

PI/PD NAME
Sharon L Vadas

ORG. REP. NAME*

FOR NSF USE ONLY		
INDIRECT COST RATE VERIFICATION		
Date Checked	Date Of Rate Sheet	Initials - ORG

 ***ELECTRONIC SIGNATURES REQUIRED FOR REVISED BUDGET**

SUMMARY PROPOSAL BUDGET COMMENTS - Year 2

**** I- Indirect Costs**
Overhead (Rate: 43.0000, Base 72437)

SUMMARY PROPOSAL BUDGET

YEAR 3

FOR NSF USE ONLY		
PROPOSAL NO.	DURATION (months) Proposed	Granted
AWARD NO.		

ORGANIZATION
NorthWest Research Associates, Incorporated

PRINCIPAL INVESTIGATOR / PROJECT DIRECTOR
Sharon L Vadas

A. SENIOR PERSONNEL: PI/PD, Co-PI's, Faculty and Other Senior Associates (List each separately with title, A.7. show number in brackets)	NSF Funded Person-months CAL	ACAD	SUMR	Funds Requested By proposer	Funds granted by NSF (if different)
1. **Sharon L Vadas - PI**	4.10	0.00	0.00	**49,338**	
2. **Erich Becker - Co-PI**	0.50	0.00	0.00	**5,495**	
3.					
4.					
5.					
6. (**0**) OTHERS (LIST INDIVIDUALLY ON BUDGET JUSTIFICATION PAGE)	0.00	0.00	0.00	**0**	
7. (**2**) TOTAL SENIOR PERSONNEL (1 - 6)	4.60	0.00	0.00	**54,833**	
B. OTHER PERSONNEL (SHOW NUMBERS IN BRACKETS)					
1. (**0**) POST DOCTORAL SCHOLARS	0.00	0.00	0.00	**0**	
2. (**0**) OTHER PROFESSIONALS (TECHNICIAN, PROGRAMMER, ETC.)	0.00	0.00	0.00	**0**	
3. (**0**) GRADUATE STUDENTS				**0**	
4. (**0**) UNDERGRADUATE STUDENTS				**0**	
5. (**0**) SECRETARIAL - CLERICAL (IF CHARGED DIRECTLY)				**0**	
6. (**0**) OTHER				**0**	
TOTAL SALARIES AND WAGES (A + B)				**54,833**	
C. FRINGE BENEFITS (IF CHARGED AS DIRECT COSTS)				**17,601**	
TOTAL SALARIES, WAGES AND FRINGE BENEFITS (A + B + C)				**72,434**	
D. EQUIPMENT (LIST ITEM AND DOLLAR AMOUNT FOR EACH ITEM EXCEEDING $5,000.)					
TOTAL EQUIPMENT				**0**	
E. TRAVEL 1. DOMESTIC (INCL. U.S. POSSESSIONS)				**3,180**	
2. INTERNATIONAL				**0**	
F. PARTICIPANT SUPPORT COSTS					
1. STIPENDS $ **0**					
2. TRAVEL **0**					
3. SUBSISTENCE **0**					
4. OTHER **0**					
TOTAL NUMBER OF PARTICIPANTS (**0**) TOTAL PARTICIPANT COSTS				**0**	
G. OTHER DIRECT COSTS					
1. MATERIALS AND SUPPLIES				**0**	
2. PUBLICATION COSTS/DOCUMENTATION/DISSEMINATION				**4,060**	
3. CONSULTANT SERVICES				**0**	
4. COMPUTER SERVICES				**1,119**	
5. SUBAWARDS				**0**	
6. OTHER				**0**	
TOTAL OTHER DIRECT COSTS				**5,179**	
H. TOTAL DIRECT COSTS (A THROUGH G)				**80,793**	
I. INDIRECT COSTS (F&A)(SPECIFY RATE AND BASE) **General and Administrative (Rate: 16.0000, Base: 111940) (Cont. on Comments Page)**					
TOTAL INDIRECT COSTS (F&A)				**49,057**	
J. TOTAL DIRECT AND INDIRECT COSTS (H + I)				**129,850**	
K. SMALL BUSINESS FEE				**0**	
L. AMOUNT OF THIS REQUEST (J) OR (J MINUS K)				**129,850**	

M. COST SHARING PROPOSED LEVEL $ **0** AGREED LEVEL IF DIFFERENT $

PI/PD NAME
Sharon L Vadas

ORG. REP. NAME*

FOR NSF USE ONLY		
INDIRECT COST RATE VERIFICATION		
Date Checked	Date Of Rate Sheet	Initials - ORG

 ***ELECTRONIC SIGNATURES REQUIRED FOR REVISED BUDGET**

SUMMARY PROPOSAL BUDGET COMMENTS - Year 3

**** I- Indirect Costs**
Overhead (Rate: 43.0000, Base 72434)

SUMMARY PROPOSAL BUDGET

Cumulative

FOR NSF USE ONLY		
PROPOSAL NO.	DURATION (months) Proposed	Granted
AWARD NO.		

ORGANIZATION
NorthWest Research Associates, Incorporated

PRINCIPAL INVESTIGATOR / PROJECT DIRECTOR
Sharon L Vadas

A. SENIOR PERSONNEL: PI/PD, Co-PI's, Faculty and Other Senior Associates (List each separately with title, A.7. show number in brackets)	NSF Funded Person-months CAL	ACAD	SUMR	Funds Requested By proposer	Funds granted by NSF (if different)
1. **Sharon L Vadas - PI**	12.60	0.00	0.00	**148,399**	
2. **Erich Becker - Co-PI**	1.50	0.00	0.00	**16,095**	
3.					
4.					
5.					
6. ( ) OTHERS (LIST INDIVIDUALLY ON BUDGET JUSTIFICATION PAGE)	0.00	0.00	0.00	**0**	
7. (**2**) TOTAL SENIOR PERSONNEL (1 - 6)	14.10	0.00	0.00	**164,494**	
B. OTHER PERSONNEL (SHOW NUMBERS IN BRACKETS)					
1. (**0**) POST DOCTORAL SCHOLARS	0.00	0.00	0.00	**0**	
2. (**0**) OTHER PROFESSIONALS (TECHNICIAN, PROGRAMMER, ETC.)	0.00	0.00	0.00	**0**	
3. (**0**) GRADUATE STUDENTS				**0**	
4. (**0**) UNDERGRADUATE STUDENTS				**0**	
5. (**0**) SECRETARIAL - CLERICAL (IF CHARGED DIRECTLY)				**0**	
6. (**0**) OTHER				**0**	
TOTAL SALARIES AND WAGES (A + B)				**164,494**	
C. FRINGE BENEFITS (IF CHARGED AS DIRECT COSTS)				**52,802**	
TOTAL SALARIES, WAGES AND FRINGE BENEFITS (A + B + C)				**217,296**	
D. EQUIPMENT (LIST ITEM AND DOLLAR AMOUNT FOR EACH ITEM EXCEEDING $5,000.)					
TOTAL EQUIPMENT				**0**	
E. TRAVEL 1. DOMESTIC (INCL. U.S. POSSESSIONS)				**9,540**	
2. INTERNATIONAL				**0**	
F. PARTICIPANT SUPPORT COSTS					
1. STIPENDS $ **0**					
2. TRAVEL **0**					
3. SUBSISTENCE **0**					
4. OTHER **0**					
TOTAL NUMBER OF PARTICIPANTS (**0**) TOTAL PARTICIPANT COSTS				**0**	
G. OTHER DIRECT COSTS					
1. MATERIALS AND SUPPLIES				**0**	
2. PUBLICATION COSTS/DOCUMENTATION/DISSEMINATION				**12,180**	
3. CONSULTANT SERVICES				**0**	
4. COMPUTER SERVICES				**3,438**	
5. SUBAWARDS				**0**	
6. OTHER				**0**	
TOTAL OTHER DIRECT COSTS				**15,618**	
H. TOTAL DIRECT COSTS (A THROUGH G)				**242,454**	
I. INDIRECT COSTS (F&A)(SPECIFY RATE AND BASE)					
TOTAL INDIRECT COSTS (F&A)				**147,180**	
J. TOTAL DIRECT AND INDIRECT COSTS (H + I)				**389,634**	
K. SMALL BUSINESS FEE				**0**	
L. AMOUNT OF THIS REQUEST (J) OR (J MINUS K)				**389,634**	

M. COST SHARING PROPOSED LEVEL $ **0** AGREED LEVEL IF DIFFERENT $

PI/PD NAME
Sharon L Vadas

ORG. REP. NAME*

FOR NSF USE ONLY		
INDIRECT COST RATE VERIFICATION		
Date Checked	Date Of Rate Sheet	Initials - ORG

C ***ELECTRONIC SIGNATURES REQUIRED FOR REVISED BUDGET**

Budget and Cost Justification for Proposal NWRA-18-P509

The total price, as documented in the following budget forms and supporting schedules, is:

Year 1:	$129,898
Year 2:	$129,886
Year 3:	$129,850
TOTAL	**$389,634**

This project is estimated to begin on 1 June 2018 and end on 31 May 2021.

For questions of a technical nature, please contact Dr. Vadas at vasha@nwra.com or (303) 415-9701 x202. For questions of a contractual nature, please contact Ms. Dana Marie Shay, Manager of Contracts and Grants, at contracts-grants@nwra.com or (425) 556-9055, ext. 310.

DIRECT COSTS

Labor Estimates:

In order to manage the project, run the body force and ray trace models, model the excitation and propagation of secondary and tertiary GWs, determine the intrinsic parameters of the extracted GOCE GWs, and take the lead role in writing the papers, it is necessary for the success of this project for PI Vadas to work for approximately 4.2 person-months per year on this project. In order to analyze MW events in the KMCM data and to help write the papers, it is necessary for Co-I Becker to work for approximately 0.5 person-months per year on this project. The costs for PI-Vadas and Co-I Becker are listed in the respective budget sections of this proposal.

NorthWest Research Associates requires all Principal Investigators to obtain external grants or contracts to fund themselves, except for a component of indirect time allowed by NWRA for writing proposals and other indirect activity. Their position at NWRA is similar to research faculty at a university or research institution.

Labor-hour estimates were obtained by planning the staffing requirements for the anticipated tasks. Time spent by personnel on bid and proposal and other indirect activity is not charged to contracts as direct salary; such time is included in indirect rates, as are secretarial and administrative support.

Labor Rates:

NWRA performs an annual salary review with salaries adjusted in January of each year and effective through 31 December. Increases are consistent with national and local cost-of-living plus merit and industry averages. For 2014 through 2018 the average salary and IRS Section 125 Cafeteria Wage[1] adjustments for the NWRA technical staff are given in Table 1.

TABLE 1

Average Base Salary and IRS Section 125 Cafeteria Wage[1] Adjustments for NWRA Technical Staff

Year Starting	Base Salary	IRS Section 125 Cafeteria Wage
Jan. 1, 2014	1.63%	11.15%
Jan. 1, 2015	1.95%	3.01%
Jan. 1, 2016	1.03%	10.46%
Jan. 1, 2017	1.68%	4.40%
Jan. 1, 2018	1.94%	3.86%

The five-year-average base salary and cafeteria wage adjustments are 1.6% and 6.6%, respectively. We will use these averages for the Base Salary and IRS Section 125 Cafeteria Wage escalation rates.

Travel Estimates:

In order to disseminate the results of this research to the community, it is necessary for PI Vadas to attend the CEDAR workshop every year. The budget for these trips include airfare (estimated at $500/workshop), a registration fee of $450/workshop, auto rental for 5 days/workshop at $70/day, and per diem for 5 days/workshop at $376/day.

Travel rates proposed reflect those quoted as the early-booked, most direct, coach-class air transportation fares available. NWRA makes every effort to book travel with carriers at the least expensive rate available at the time and to take advantage of discounts when feasible. Per diem and hotel rates are used in accordance with the Federal Travel Regulations for CONUS and Joint Travel Regulations.

Computer Service Center:

Our basis for allocating our Computer Service Center costs is labor hours expended by computer users. The operating cost of each workstation within the computer service center is allocated based on the labor hours of the individual assigned to the workstation. Each employee has a unique hourly computer rate that depends on their actual and estimated computer costs.

Other Direct Costs:

In order to disseminate the results of this research, it is necessary for the success of this project for PI Vadas to publish 1 paper per year in peer-reviewed journals. The estimated number of published pages per year is 28, and we estimate the cost to be $145/page.

Other direct costs in this project are based on historically known costs for the same or like items.

INDIRECT COSTS

Fringe Benefit, Overhead and G&A Rates:

For reference, three years of past indirect rates are given in Table 2.

TABLE 2

Indirect Rates from previous years

Year	Fringe	Overhead	G&A
2015	32.00%	43.10%	16.00%
2016*	32.10%	43.85%	16.00%
2017*	32.10%	43.85%	16.00%

*pending final DCAA audit

The approved provisional billing rates from 1 January 2018 through the entire period of performance are: Fringe Benefits[1] – 32.10%, Overhead – 43.00%, G&A – 16.00%. On consultant and subcontract costs an 8.50% G&A rate is direct charged; these costs are exempt from the regular 16.00% G&A rate charge.

ADMINISTRATIVE INFORMATION

NWRA has a complete set of financial and cost records to substantiate all figures in this proposal. Our cognizant audit agency is DCAA Rainier Branch. The auditor supervisor is Mr. Ryan Mavin, who can be reached at 425-793-3834. Our DCMA ACO is Mr. Donald Rider, who can be reached at (425) 463-4127.

These cost estimates are in effect for 120 days from the date of this proposal.

---

[1] The IRS Section 125 Cafeteria Wage is provided by NWRA to compensate employees for IRS Section 125 pre-tax deductible health insurance premiums; it is included in an employee's W2 income and therefore part of an employee's direct labor rate. Health-insurance premiums are not included in fringe benefits.

CURRENT AND PENDING SUPPORT:

Sharon L. Vadas

Project/Proposal Title: This Proposal: Collaborative Research: Modeling of secondary and tertiary gravity waves from orographic gravity wave forcing and comparison with satellite observations Source of Support: NSF Aeronomy **Status: Pending** Total Award Amount: $389,634 Total Award Period Covered: 06/01/18 - 05/31/21 Location of Project: NWRA, CoRA Office Person-Months Per Year Committed to the Project: Cal: 4.2
Project/Proposal Title: Collaborative Research: Characterizing Secondary Gravity Waves and Influences on Momentum Transport Source of Support: NSF Aeronomy **Status: Pending** Total Award Amount: $68,674 Total Award Period Covered: 07/01/18-06/30/21 Location of Project: NWRA, CoRA Office Person-Months Per Year Committed to the Project: Cal: 0.9
Project/Proposal Title: Collaborative Research: Secondary gravity waves in the upper mesosphere and lower thermosphere Source of Support: NSF Aeronomy **Status: Pending** Total Award Amount: $389,806 Total Award Period Covered: 06/01/18-05/31/21 Location of Project: NWRA, CoRA Office Person-Months Per Year Committed to the Project: Cal: 0.49
Project/Proposal Title: Investigation of gravity waves from deep convection as a source of the small-scale structure in the O2 airglow measured by HRDI Source of Support: NASA HSR **Status: Pending** Total Award Amount: $749,846 Total Award Period Covered: 06/01/18-05/31/21 Location of Project: NWRA, CoRA Office Person-Months Per Year Committed to the Project: Cal: 4.0
Project/Proposal Title: Collaborative Research: Fe and Na Lidar Investigation of Middle and Upper Atmosphere Temperature, Composition, Dynamics, and Chemistry (30-200 km) at McMurdo, Antarctica Source of Support: NSF Division of Polar Programs, Antarctic Research **Status: Pending** Total Award Amount: $131,613 Total Award Period Covered: 09/01/18-08/31/23 Location of Project: NWRA, CoRA Office Person-Months Per Year Committed to the Project: Cal: 1.0

Project/Proposal Title: Collaborative Research: Lidar Investigation of Middle and Upper Atmosphere Temperature, Composition, Chemistry and Dynamics at McMurdo, Antarctica
Source of Support: NSF OPP/Antarctic Research Program Status: Current
Total Award Amount: $95,307 Total Award Period Covered: 09/01/13-08/31/18
Location of Project: NWRA, CoRA Office
Person-Months Per Year Committed to the Project: Cal: 0.72
Project/Proposal Title: Collaborative Research: CEDAR--Modeling and observation of secondary gravity waves in the thermosphere and ionosphere generated from deep convection
Source of Support: NSF CEDAR Status: Current
Total Award Amount: $355,367 Total Award Period Covered: 06/01/16 - 05/31/19
Location of Project: NWRA, CoRA Office
Person-Months Per Year Committed to the Project: Cal: 4.5

NOTE: Awards with period of performance dates highlighted in yellow will EXPIRE within 3 months of the start of the proposed period of performance.

CURRENT AND PENDING SUPPORT:
Erich Becker

Pending:

Project/Proposal Title: This Proposal: Collaborative Research: Modeling of secondary and tertiary gravity waves from orographic gravity wave forcing and comparison with satellite observations Source of Support: NSF Aeronomy Total Award Amount: $389,634 Total Award Period Covered: 06/01/18 - 05/31/21 Location of Project: NWRA, CoRA Office Person-Months Per Year Committed to the Project: Cal: 0.5
Project/Proposal Title: Collaborative Research: Secondary gravity waves in the upper mesosphere and lower thermosphere Source of Support: NSF Aeronomy Total Award Amount: $389,806 Total Award Period Covered: 06/01/18-05/31/21 Location of Project: NWRA, CoRA Office Person-Months Per Year Committed to the Project: Cal: 4.5

Current:

None

*Erich Becker is employed at the Leibniz Institute of Atmospheric Physics (IAP) in Germany as a department head and is a professor at the University of Rostock. His position is permanent and part of the regular budget of IAP. However, he wants to move to the US and work as a scientist at NWRA. To become an employee at NWRA requires that the necessary funding of research proposals is approved. Erich Becker has not been on a project or applied for funding in the US in the past.

NorthWest Research Associates' Facilities and Equipment Statement

NorthWest Research Associates (NWRA, www.nwra.com) is a small scientific research organization owned and operated by its Principal Investigators, with expertise in the space and geophysical sciences. Focused areas in basic and applied research include, but are not limited to: fundamental fluid dynamics, atmospheric science, ionospheric, solar, and stellar physics, oceanography, sea-ice mechanics, and electromagnetism. NWRA has 70 employees with offices in three locations:

- **Seattle Area, WA**

  Home of NWRA Headquarters and the Seattle-area scientists, the office is located near the Redmond campus of Microsoft, directly across Lake Washington from the University of Washington on an express bus line.

- **Boulder, CO**.

  The Boulder science office, also known as CoRA, is located adjacent to the NCAR Foothills Lab, and 2 miles from Space, Atmosphere, and Ocean Sciences facilities at the University of Colorado East Campus.

- **Monterey, CA**.

  The Monterey science facility is in downtown Monterey with 2750 square feet of office space, approximately 0.5 miles from the Naval Postgraduate School.

NWRA also employs individual researchers who work in the following areas: Corvallis, OR; San Diego, CA; and Socorro, NM.

The research described in this proposal will be performed at NWRA's facility located in Boulder, Colorado. This facility provides the scientists with the latest in computing and networking technology infrastructure. Scientists define their own personal computing platform to best meet their individual needs. Several scientists have additional offsite High Performance Computing (HPC) accounts. Networking servers and data acquisition servers are housed in a protected and separately cooled server room. Daily and monthly backups, with offsite storage, and closely monitored firewalls, provide protection and security.

Data Management Plan

Types of data, samples, physical collections, software, curriculum materials, and other materials to be produced in the course of the project:

Modeling data created by this project are 1) the body forces from mountain wave breaking over the Southern Andes, the Antarctic Peninsula, and the Rocky Mountains, 2) the thermospheric body forces from secondary gravity wave dissipation, and 3) the spectra of secondary and tertiary gravity waves in the thermosphere as functions of altitude, latitude and longitude. We anticipate that the total amount modeling data will be approximately 100 GB for the duration of this project.

Byproducts of analyzed observational data created by this project will be the extracted gravity wave spectra from the GOCE data over the Southern Andes and Rocky Mountains. These gravity wave spectra will contain their amplitudes, intrinsic parameters and directions of propagation. We estimate that we will have analyzed approximately 100-200 gravity waves total. We anticipate a total amount of data of approximately 1 MB for the duration of this project.

Standards to be used for data and metadata format and content (where existing standards are absent or deemed inadequate, this should be documented along with any proposed solutions or remedies):

The model results will be available in ascii or binary format. Instructions will be included with the model results for reading the files.
All gravity waves from the GOCE data will saved as ascii files with header information accompanying the numerical data files.

There will be no metadata sets as part of this project.

Policies for access and sharing including provisions for appropriate protection of privacy, confidentiality, security, intellectual property, or other rights or requirements:

Model and GOCE analyses results will be kept private until the corresponding paper(s) has been accepted by a scientific journal or 2 years after the end of the grant (whichever comes first). After that time, the GOCE GWs and model data will be made available to other researchers and to the general public via an email request to Dr. Vadas at vasha@cora.nwra.com.

Policies and provisions for re-use, re-distribution, and the production of derivatives:

We would like to be consulted prior to re-use, re-distribution, and production of the derivatives of the model and GOCE gravity wave results.

Plans for archiving data, samples, and other research products, and for preservation of access to them.

The model and GOCE gravity wave results will be stored for at least 5 years on the computers at NWRA/CoRA in Boulder, CO. There are no plans to delete this data.